AD-773 713

RANGE LAWS FOR FM RADARS WITH HARMONIC
PROCESSING AND ARBITRARY MODULATING
WAVESHAPES

Leon W. Couch, et al

Florida University

DOCUMENT CONTROL DATA - R & D

Security classification of title, body of abstract and indexing annotation must be entered when the overall report is classified)

1. ORIGINATING ACTIVITY (Corporate author)	2a. REPORT SECURITY CLASSIFICATION
ENGINEERING AND INDUSTRIAL EXPERIMENT STATION UNIVERSITY OF FLORIDA GAINESVILLE, FLORIDA 32601	UNCLASSIFIED
	2b. GROUP

3. REPORT TITLE

RANGE LAWS FOR FM RADARS WITH HARMONIC PROCESSING AND ARBITRARY MODULATING WAVESHAPES

4. DESCRIPTIVE NOTES (Type of report and inclusive dates)

5. AUTHOR(S) (First name, middle initial, last name)

Leon W. Couch
Raymond C. Johnson

6. REPORT DATE	7a. TOTAL NO. OF PAGES	7b. NO. OF REFS
November 14, 1973	50	13

8a. CONTRACT OR GRANT NO	9a. ORIGINATOR'S REPORT NUMBER(S)
DAAG39-73-C-0169	
b. PROJECT NO	0169-1
HDL Proj: 10131J	
c. DA-1B262301A208	9b. OTHER REPORT NO(S) (Any other numbers that may be assigned this report)
d. AMCMS Code: 522A.11.17700	

10. DISTRIBUTION STATEMENT

This document has been approved for public release and sale;
its distribution is unlimited.

11. SUPPLEMENTARY NOTES	12. SPONSORING MILITARY ACTIVITY
	ARMY MATERIEL COMMAND HARRY DIAMOND LABORATORIES WASHINGTON, D. C. 20438

13. ABSTRACT

The range response of a periodically modulated FM radar is derived for some useful harmonic processing systems in terms of Fourier coefficients which are identical to points on the ambiguity function. The Fourier coefficients are evaluated for a piecewise-linear modulation waveform which may be used to approximate an arbitrary modulating waveshape. Thus, the approximate range response of an arbitrary modulation waveform is obtained. Range laws for incoherent, coherent and directional doppler detection are obtained by vector addition of the properly weighted complex Fourier coefficients. For coherent harmonic processing using an arbitrary periodic waveform for the reference, the phasing of the reference waveform is shown to be of importance in cancelling undesired range sidelobes.

Examples of computed and measured range responses are included which show improved range sidelobe suppression--up to 30dB--for types of modulation and demodulation schemes which are particularly suited to digital implementation.

DD FORM 1473 REPLACES DO FORM 1473, 1 JAN 64, WHICH IS
1 NOV 65 OBSOLETE FOR ARMY USE

UNCLASSIFIED

DA-1B262301A208
AMCMS Code: 522A.11.17700   AD_____
HDL Proj: 10131J

0169-1

RANGE LAWS FOR FM RADARS WITH HARMONIC

PROCESSING AND ARBITRARY MODULATING WAVESHAPES

by

L. W. Couch
R. C. Johnson

November 14, 1973

United States Army Materiel Command

HARRY DIAMOND LABORATORIES

Washington, D. C. 20439

TABLE OF CONTENTS

Pages 3 and 4 are Blank

KEY TO SYMBOLS

B Peak-to-peak FM deviation (Hz)

c_k Fourier coefficient of $v(t)v^*(t-\tau)$. This is identical to a section of the ambiguity function cut perpendicular to the frequency axis at the frequency $k\omega_m$--see(12b)

D Deviation sensitivity of the FM modulator (radian/sec-volt)

$m(t)$ Periodic frequency modulating waveform

$r(t)$ Periodic reference signal used for coherent detection

r_k Fourier coefficient for the kth harmonic of the periodic reference signal

$R_n(\tau)$ Range response obtained by doppler processing about the nth harmonic of the modulation frequency

$v(t) = e^{jD_0\int^t m(t)dt}$ Complex envelope of the radiated RF signal

$x = 2B\tau$ Normalized round-trip time delay between the radar and the target

$y(t,\tau)$ Mixer output signal

$y_{det}(t,\tau)$ Processed doppler output signal

$z_n(\tau)$ Complex envelope of the processed doppler signal obtained by detection about the nth harmonic of the modulation frequency

$\theta_d(t,\tau)$ Difference phase between the transmitted and received RF signals

$\omega_c = 2\pi f_c$ Radian carrier frequency

$\omega_d = 2\pi f_d$ Radian doppler frequency

$\omega_{id}(t,\tau) = \dfrac{d\theta_d(t,\tau)}{dt}$ Instantaneous difference frequency (rad/sec) between the transmitted and received RF signals

$\omega_m = 2\pi f_m = \dfrac{2\pi}{T}$ Fundamental modulating frequency (rad/sec)

$\omega_r = n\omega_m$ Fundamental frequency of the periodic reference signal. This is the nth harmonic of the modulating signal

RANGE LAWS FOR FM RADARS WITH HARMONIC

PROCESSING AND ARBITRARY MODULATING WAVESHAPES

1. INTRODUCTION

The range response or range laws* for FM radars with arbitrary modulating-signal waveshapes are examined in this report. The range law depends on the type of processing that is used as well as the modulating-signal waveshape.

It is assumed that the modulating signal is periodic so that the video output of the radar is periodic with energy concentrated about harmonics of the modulating frequency. By detecting the signal in these harmonics, range laws are obtained. The particular range law that is obtained will depend on (1) the frequency-modulating-signal waveshape, (2) the harmonic number that is detected and (3) whether the harmonic energy is coherently or incoherently detected. If coherent processing is used, the range law also depends on the waveshape of the reference signal (e.g. sinusoidal or square-wave) and on the phase angle of the reference with respect to the modulating waveform.

Harmonic processing is desirable because the range laws can be made to peak up at non-zero distances from the target. This eliminates the need for a delay line. A single antenna may be used for both transmission and reception if the incidental AM is sufficiently small. Thus, harmonic processing gives a low cost radar.

Range laws with low sidelobe-levels are desired for good target resolution. Here it is desired to find the modulating-signal waveshape and harmonic processing system which in combination will yield the best range laws (i.e. maximum sidelobe suppression). In choosing the best combination to use, hardware considerations are important, since there are many waveforms and harmonic processing schemes which yield equally good range laws, but some are more expensive to implement than others.

A nonlinear modulating waveform which gives 30dB of sidelobe suppression is well-known [1,2,3]. However, the range law peaks up at zero and consequently is not useful unless delay lines are used in the radar. The triangular modulating waveform is often used because of economic consideration but the sidelobe ratio is less than 14dB for harmonic processing [4,5,6]. Here we propose systems which are economically competitive with the triangular FM system but which offer much better sidelobe suppression, up to 30dB.

As indicated above, the response of the harmonic system depends on the type of processing that is used, such as incoherent, coherent, or single-sideband. In this report, the exact range response of these systems is derived in terms of

---

*The range law of the radar is the envelope (or amplitude) of the doppler signal as a function of the round-trip time delay to an ideal point target, neglecting the space loss.

Fourier coefficients of the complex envelope of the post-mixer spectrum. These coefficients are identical to the value of the ambiguity function at the corresponding harmonic frequency and round-trip time delay to the target. Consequently, if the ambiguity function for the modulating signal is known, the response of these harmonic processers is known via these formulas.

Tozzi has analyzed harmonic FM systems with linear and sinusoidal modulating waveforms [5]. For the linear case his analysis included the effect of the "turn around" time. In this report the Fourier coefficients are derived for a modulating waveshape consisting of an arbitrary number of linear segments, neglecting the "turn-around" effect. This waveform may be used to approximate an arbitrary modulating waveshape (linear or nonlinear) by specifying a set of parameters. Using these Fourier coefficients in the formula for the appropriate processing system, the approximate range law for a particular processing system and modulating waveshape is obtained. Since the "turn-around" time is neglected in the piecewise-linear model these results are valid when the round trip time delay is much smaller than the duration of any of the segments of the piecewise waveform.

In summary, the range law is derived for some useful FM harmonic processing systems in terms of Fourier coefficients which are identical to points on the ambiguity function. The Fourier coefficients are evaluated for a piecewise-linear modulation waveform which may be used to approximate an arbitrary modulating waveshape. Examples of new nonlinear waveforms are given which, when used with the proper processing, give range responses with 30dB sidelobe suppression.

2. FM RADAR

An FM radar with incoherent harmonic processing is shown in Figure 1. The transmitted signal is frequency modulated by a periodic waveform. The spectrum of the mixer output is concentrated about harmonics of the modulating frequency, ω_m. The range response, or range law, is the envelope of the detector response
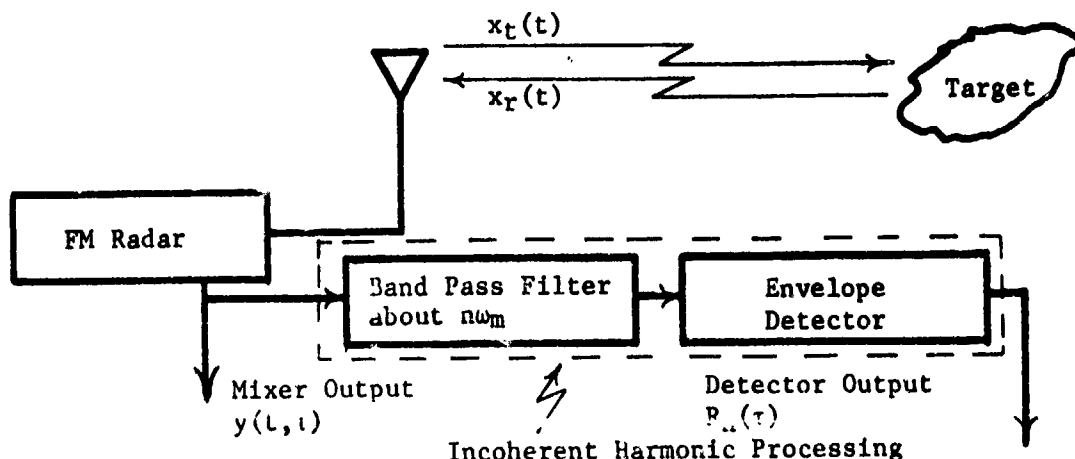

Incoherent Harmonic Processing

Figure 1. FM Radar

for a point target where τ is the round-trip time delay between the radar and the target.* It will be denoted by $R_n(\tau)$. For purely linear modulation the range law peaks up for a target spacing corresponding to a round-trip time delay of $\tau_0 = n/2B$ where B is the peak-to-peak frequency deviation (Hz). Any modulation nonlinearity will shift this τ_0 slightly and alter the side-lobe levels. If there is a doppler present the range law is the envelope of the doppler signal. The processing is of the matched filter type for n=0, or for any value of n if the modulation is purely linear.

For periodic modulation the range law is obtained by evaluating the Fourier coefficient for the mixer output of the radar. Referring to Figure 1, the transmitted signal is represented by

$$x_t(t) = \sqrt{2} \; \text{Re} \; \{v(t)e^{j\omega_c t}\} \tag{1}$$

where ω_c is the radian carrier frequency and $v(t)$ is the complex envelope [7]. Then the corresponding received signal is

$$x_r(t) = \sqrt{2} \; \text{Re} \; \{v(t-\tau)e^{j\omega_c(t-\tau)}\} \tag{2}$$

where τ is the round trip time delay.

To the first approximation, the mixer output is given by the cross-product term

$$y(t,\tau) = \text{Re} \; \{v(t)v*(t-\tau)e^{j\omega_c \tau}\} \tag{3}$$

where the output about $2\omega_c$ has been neglected since it is filtered out.

For a frequency modulated radar

$$v(t) = e^{j[D_0 \int^t m(t)dt]}$$

where D is the deviation sensitivity (radians/volt-sec) and $m(t)$ is the periodic frequency modulating waveform. Then

$$v(t)v*(t-\tau) = e^{j\theta_d(t,\tau)} \tag{4}$$

where

$$\theta_d(t,\tau) = D \int_{t-\tau}^{t} m(\sigma)d\sigma \; . \tag{4a}$$

$\theta_d(t,\tau)$ is the mixer output difference phase with τ being a parameter.

The instantaneous difference radian frequency associated with the mixer output is then

$$\omega_{id}(t,\tau) = \frac{d\theta_d(t,\tau)}{dt} = D[m(t) - m(t-\tau)] \tag{5}$$

---

*The range law of the radar is defined as the radar response (in this radar $R_n(\tau)$) as a function of the round-trip time delay to an ideal point target, neglecting the space loss. This gives the range resolution capability of the radar and, for the n=0 case, is the magnitude of the autocorrelation function associated with the transmitted spectrum. In Figure 1 a constant closing velocity with respect to the target will produce a sinusoidal doppler signal at the output of the envelope detector. $R_n(\tau)$ is the amplitude (or envelope) of the doppler signal.

where it is assumed that the variation of τ with respect to t is negligible, i.e. the doppler frequency is much less than the carrier frequency. Thus,

$$\theta_d(t,\tau) = D \int_0^t [m(t) - m(t-\tau)]d\tau \quad . \tag{6}$$

Note that (6) neglects a phase constant that was included in (4a) but which was lost in (5). If m(t) is periodic, then, $\theta_d(t,\tau)$ is periodic with respect to t. Thus, from (4), $v(t)v^*(t-\tau)$ is also periodic and can be expanded in a Fourier series

$$v(t)v^*(t-\tau) = e^{j\theta_d(t,\tau)} = \sum_{k=-\infty}^{k=\infty} c_k e^{jk\omega_m t} \tag{7}$$

where

$$c_k = \frac{1}{T} \int_{-T/2}^{T/2} e^{j\theta_d(t,\tau)} e^{-jk\omega_m t} dt = \frac{1}{T} \int_{-T/2}^{T/2} v(t)v^*(t-\tau)e^{-jk\omega_m t} dt \tag{8}$$

ω_m is the angular frequency of the modulating waveform and T is the period. Thus, $\omega_m = 2\pi/T$.

Furthermore, the mixer output, as described by (3) is periodic so that

$$y(t,\tau) = \sum_{k=-\infty}^{\infty} y_k e^{jk\omega_m t} \tag{9}$$

where

$$y_k = \frac{1}{T} \int_{-T/2}^{T/2} y(t,\tau)e^{-jk\omega_m t} \quad . \tag{10}$$

Equation (10) can be related to (8) by

$$y_k = \frac{1}{2} e^{j\omega_c \tau} c_k + \frac{1}{2} e^{-j\omega_c \tau} c^*_{-k} \quad . \tag{11}$$

This explicitly shows the variation of y_k with the doppler since $\omega_c \tau = \omega_d t + \phi_0$ where ω_d is the radian doppler frequency. ϕ_0 is the phase angle of the doppler at t=0 and we will assume that $\phi_0=0$ for mathematical simplicity.

It is interesting to note that the $\{c_k\}$ are related directly to the ambiguity function. If Helstrom's definition of the ambiguity function [10] is used, the relationship is [6]

$$c_k(\tau) = e^{j\frac{k\omega_m \tau}{2}} \lambda(-\tau, k\omega_m) \quad . \tag{12a}$$

10

Using Woodward's definition [11], the relationship is

$$\boxed{c_k(\tau) = \chi(-\tau, k\omega_m)}$$ (12b)

For either of these definitions

$$|c_k(\tau)| = |\lambda(-\tau, k\omega_m)|$$ (13)

Thus [8]

$$|c_k(\tau)| \leq |c_0(0)|$$ (14)

3. INCOHERENT HARMONIC PROCESSING

Referring to Figure 1, the formula for the range law $R_n(\tau)$ will be obtained for incoherent detection of the nth harmonic component of the mixer output.

Using (9) the output of the ideal band-pass filter is

$$y_{out}(t,\tau) = y_n e^{jn\omega_m t} + y_{-n} e^{-jn\omega_m t}$$ (15)

Since $y(t,\tau)$ is a real function $y_{-n} = y_n^*$ and (15) becomes

$$y_{out}(t,\tau) = 2 \operatorname{Re} \{y_n e^{jn\omega_m t}\}$$ (16)

The output of the envelope detector is the magnitude of the complex envelope of (16):

$$y_{det}(t,\tau) = 2|y_n| = R_n(\tau)$$

$$\boxed{R_n(\tau) = |c_n e^{j\omega_c \tau} + c_{-n}^* e^{-j\omega_c \tau}|}$$ (17)

This equation cannot be reduced further unless some simplifying assumptions are made or unless $\{c_k\}$ are evaluated for a particular modulating waveshape. For example, if the instantaneous difference frequency has half-wave odd symmetry, that is if

$$\omega_{id}(t,\tau) = -\omega_{id}(t + \frac{T}{2}, \tau)$$ (18)

then $c_k = c_{-k}$ [6]. Then, (17) becomes, for $n \neq 0$,

$$y_{det}(t,\tau) = 2|c_n||\cos[\omega_d(t-t_0) + \underline{/c_n}]| , \quad n \neq 0$$ (19)

where ω_d is the radian doppler frequency and t_0 is the value of t at the first turn-around time of the modulation [6]. For $n \neq 0$, $y_{det}(t,\tau)$ is a full-wave rectified sine-wave and its envelope varies with τ to give the range response. For $n = 0$, the band-pass filter becomes a low-pass filter and the envelope detector would not be needed. Thus,

$$y_{out}(t,\tau) = |c_0| \cos[\omega_d(t-t_0) + \underline{/c_0}] \quad , \quad n = 0 \quad . \tag{20}$$

Thus, for modulating waveforms such that the difference frequency has <u>half-wave odd symmetry</u>, incoherent detection produces the range laws

$$R_r(\tau) = \begin{bmatrix} |c_0(\tau)| & , & n = 0 \\ \\ 2|c_n(\tau)| & , & n = 1,2 \cdots \end{bmatrix} \quad . \tag{21}$$

This shows that if the difference frequency has half-wave odd symmetry, the range response of the FM radar with incoherent harmonic processing is the magnitude of the ambiguity function along the τ axis where the slice is taken at $\omega = n\omega_m$ [see (13).]

4. COHERENT HARMONIC PROCESSING WITH A PERIODIC REFERENCE SIGNAL

4.1 General Periodic Reference Signal

Referring to Figure 2, the range law will now be calculated for the case of coherent detection where any periodic reference signal, $r(t)$, is used. Using these results, we will later obtain specific results for a sinusoidal reference and a square-wave reference.
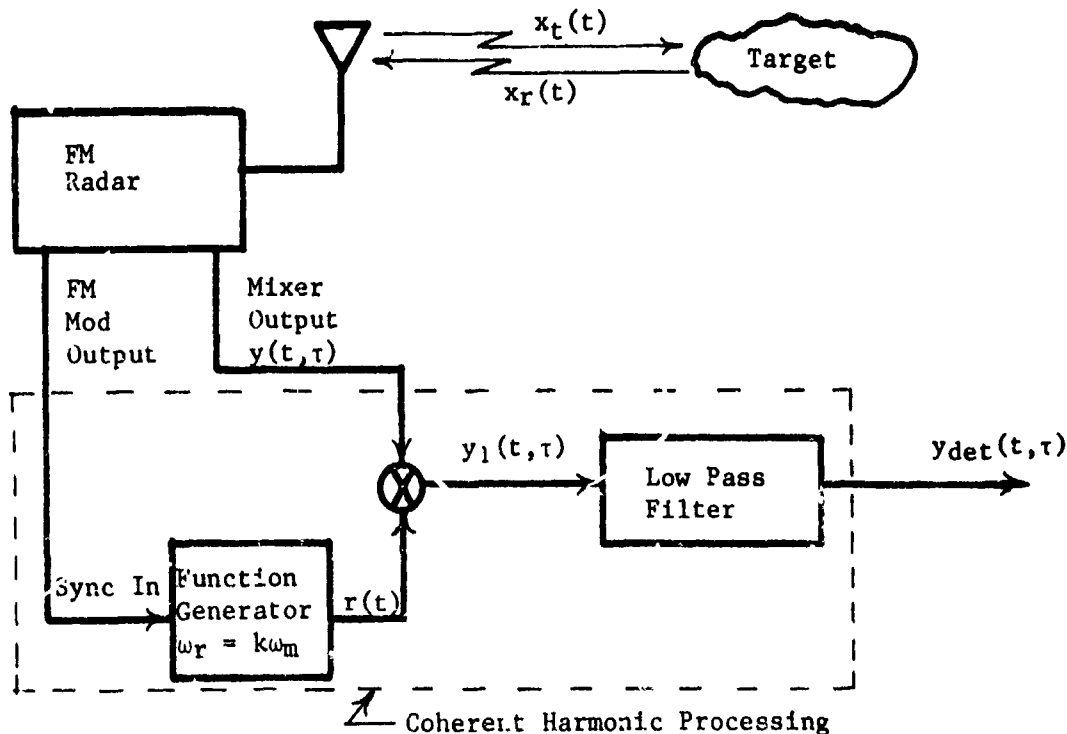

Figure 2.   FM Radar with Coherent Harmonic Processing

The periodic reference is represented by the Fourier series:

$$r(t) = \sum_{k=-\infty}^{\infty} r_k e^{jk\omega_r(t-t_0)}$$

or

$$r(t) = \sum_{k=-\infty}^{\infty} r_k e^{j(k\omega_r t + k\theta_0)} \tag{22}$$

where $\omega_r = n\omega_m$. That is, the fundamental frequency of the reference waveform is some harmonic of the fundamental of the modulation frequency. $\theta_0 = -\omega_r t_0$ is the reference phase angle, and t_0 corresponds to any time shift of the reference waveform with respect to the $t = 0$ point on the modulating-signal waveform. Note that the index k is chosen with respect to the reference frequency (not the modulating frequency).

Using (9) and (22), the multiplier output is

$$y_1(t,\tau) = y(t,\tau)r(t)$$

$$= \left[\sum_{\ell=-\infty}^{\infty} y_\ell e^{j\ell\omega_m t}\right]\left[\sum_{k=-\infty}^{\infty} r_k e^{j(k\omega_r t + k\theta_0)}\right]$$

and using $\omega_r = n\omega_m$

$$y_1(t,\tau) = \sum_{\ell=-\infty}^{\infty} \sum_{k=-\infty}^{\infty} y_\ell r_k e^{j[(nk+\ell)\omega_m t + k\theta_0]} . \tag{23}$$

The output of the low-pass filter is then

$$y_{det}(t,\tau) = \sum_{k=-\infty}^{\infty} y_{-nk} r_k e^{jk\theta_0} . \tag{24}$$

Using (11), (24) can be reduced to the form where the doppler signal is seen explicitly. Thus

$$y_{det}(t,\tau) = \sum_{k=-\infty}^{\infty} \frac{1}{2}\left[c_{-nk} e^{j\omega_c\tau} + c^*_{-nk} e^{-j\omega_c\tau}\right] r_k e^{jk\theta_0}$$

$$= \frac{1}{2}\left\{c_0 r_0 + \sum_{k=1}^{\infty} \left[c_{-nk} r_k e^{jk\theta_0} + c_{nk} r_{-k} e^{-jk\theta_0}\right]\right\} e^{j\omega_c\tau}$$

$$+ \frac{1}{2}\left\{c^*_0 r_0 + \sum_{k=1}^{\infty} \left[c^*_{nk} r_k e^{jk\theta_0} + c^*_{-nk} r_{-k} e^{-jk\theta_0}\right]\right\} e^{-j\omega_c\tau} \tag{25}$$

Since $r(t)$ is a real function $r_{-k} = r_k^*$ and since $2\text{Re}\{a+jb\} = [a+jb] + [a+jb]^*$, then

$$y_{\det}(t,\tau) = \text{Re}\left[\{c_0 r_0 + \sum_{k=1}^{\infty} [c_{-nk} r_k e^{jk\theta_0} + c_{nk} r_{-k} e^{-jk\theta_0}]\} e^{j\omega_c \tau}\right] \qquad (26)$$

Define

$$z_n \triangleq c_0 r_0 + \sum_{k=1}^{\infty} [c_{-nk} r_k e^{jk\theta_0} + c_{nk} r_{-k} e^{-jk\theta_0}]$$

$$= c_0 r_0 + \sum_{k=1}^{\infty} c_{-nk} r_k e^{jk\theta_0} + \sum_{k=-\infty}^{k=-1} c_{-nk} r_k e^{jk\theta_0} \qquad . \qquad (27)$$

Thus,

$$y_{\det}(t,\tau) = |z_n| \cos\{\omega_c \tau + \underline{/z_n}\} \qquad (28)$$

$$z_n(\tau) = \sum_{k=-\infty}^{\infty} c_{(-nk)}(\tau) r_k e^{jk\theta_0} \qquad (29)$$

where $|z_n|$ denotes the magnitude of $z_n(\tau)$

$\underline{/z_n}$ denotes the angle of $z_n(\tau)$

$\{r_k\}$ are the Fourier coefficients of the periodic reference waveform

$\{c_\ell\}$ are the Fourier coefficients of $v(t)v^*(t-\tau)$ where $v(t)$ is the complex envelope of the FM signal [see (8) and (51)] and $\ell = -nk$

and θ_0 is the phase angle of the fundamental of the periodic reference signal with respect to the $t = 0$ point of the modulating signal. The $\{c_\ell\}$ are also directly related to a section of the ambiguity function taken along the axis at the frequency $\omega = \ell\omega_m$. That is, referring to (12b)

$$c_\ell(\tau) = \chi(-\tau, \ell\omega_m) \qquad (30)$$

Equation (28) explicitly shows the doppler signal phase since $\omega_c \tau = \omega_d t$ where ω_d is the radian doppler frequency.

The range law for coherent harmonic processing is given by the envelope of the doppler signal, which is

$$R_n(\tau) = |z_n(\tau)| \qquad (31)$$

where the n denotes that this particular range response is obtained when the fundamental frequency of the reference signal is the nth harmonic of the modulation frequency, $\omega_r = n\omega_m$. From (29), (30) and (31), it is evident that the range response is obtained by the superposition of sections of the ambiguity

function with appropriate complex-weighting factors.

4.2 Sinusoidal Reference Signal

To coherently process the doppler signal about the nth harmonic of the mixer output, the reference signal is

$$r(t) = \cos [n\omega_m t + \theta] = \cos [\omega_r t + \theta] \qquad (32)$$

or

$$r(t) = \frac{1}{2} e^{j[\omega_r t + \theta]} + \frac{1}{2} e^{-j[\omega_r t + \theta]} \qquad (33)$$

where $\omega_r = n\omega_m$. Thus, the Fourier coefficients in (22) become

$$r_k = \begin{bmatrix} \frac{1}{2} , \text{ for } |k| = 1 \\ \\ 0 , \text{ for } |k| \neq n \end{bmatrix} \qquad (34)$$

Using (29) and (31), the range law for coherent detection about the nth harmonic of the modulation frequency (i.e. sinusoidal reference) is

$$R_n(\tau) = |z_n(\tau)| \qquad (35)$$

where

$$z_n(\tau) = \frac{1}{2} [c_{-n}(\tau) e^{j\theta} + c_n(\tau) e^{-j\theta}] \qquad (36)$$

4.3 Square Wave (Gating) Reference Signal

A square wave (gating) reference signal with a period of T/n is shown below.

15
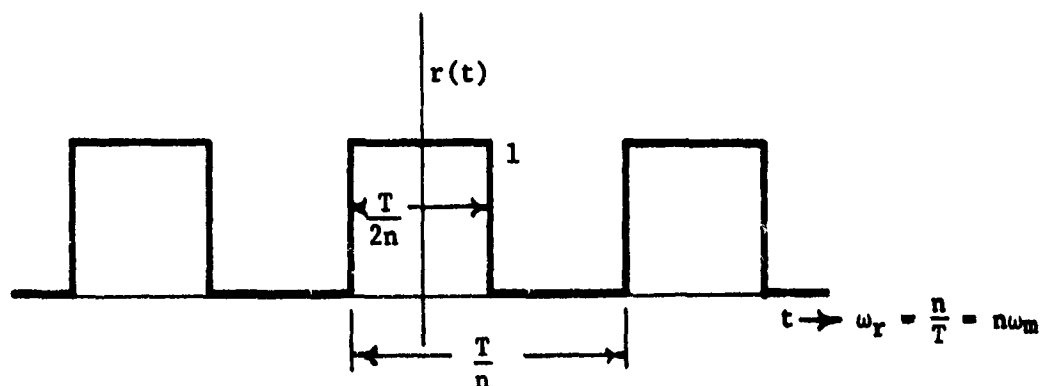
The Fourier coefficients are,

$$r_k = \frac{1}{2} \frac{\sin (k\pi/2)}{k\pi/2} \tag{37}$$

Using (29) and (31), the range law for coherent detection using a square wave reference is

$$R_n(\tau) = |z_n(\tau)| \tag{38}$$

where

$$z_n(\tau) = \sum_{k=-\infty}^{\infty} c_{-nk}(\tau) \; \frac{1}{2} \frac{\sin (k\pi/2)}{k\pi/2} \; e^{jk\theta_0} \tag{39a}$$

or

$$z_n(\tau) = \cdots - \frac{1}{3\pi} c_{-3n}(\tau) e^{-j3\theta_0} + \frac{1}{\pi} c_{-n}(\tau) e^{-j\theta_0} + \frac{1}{2} c_0(\tau) + \frac{1}{\pi} c_n(\tau) e^{j\theta_0}$$

$$- \frac{1}{3\pi} c_{3n}(\tau) e^{j3\theta_0} \cdots \tag{39b}$$

5. SINGLE-SIDEBAND PROCESSING FOR DIRECTIONAL DOPPLER DETECTION

The range law will be calculated for single-sideband (SSB) processing of the mixer output signal as shown in Figure 3. By using the appropriate modulating waveform, range laws can be obtained which peak up either for approaching or receding targets.

Using (7) in (3), the mixer output is

$$y(t,\tau) = \sum_{k=-\infty}^{+\infty} \text{Re}\{c_k e^{j(k\omega_m + \omega_d)t}\}$$

where $\omega_c \tau = \omega_d t$. ω_d is the doppler frequency. It is positive for receding targets and negative for approaching targets. The output of the sideband filter is

$$y_1(t,\tau) = \begin{bmatrix} \text{Re}[c_{\pm n} e^{j(\pm n\omega_m + \omega_d)t}] & , & \omega_d > 0 \\ \\ \text{Re}[c_{\mp n} e^{j(\mp n\omega_m + \omega_d)t}] & , & \omega_d < 0 \end{bmatrix}$$

where the upper set of signs is used if the filter passes upper SSB signals and the lower set of signs is used if the filter passes lower SSB signals.
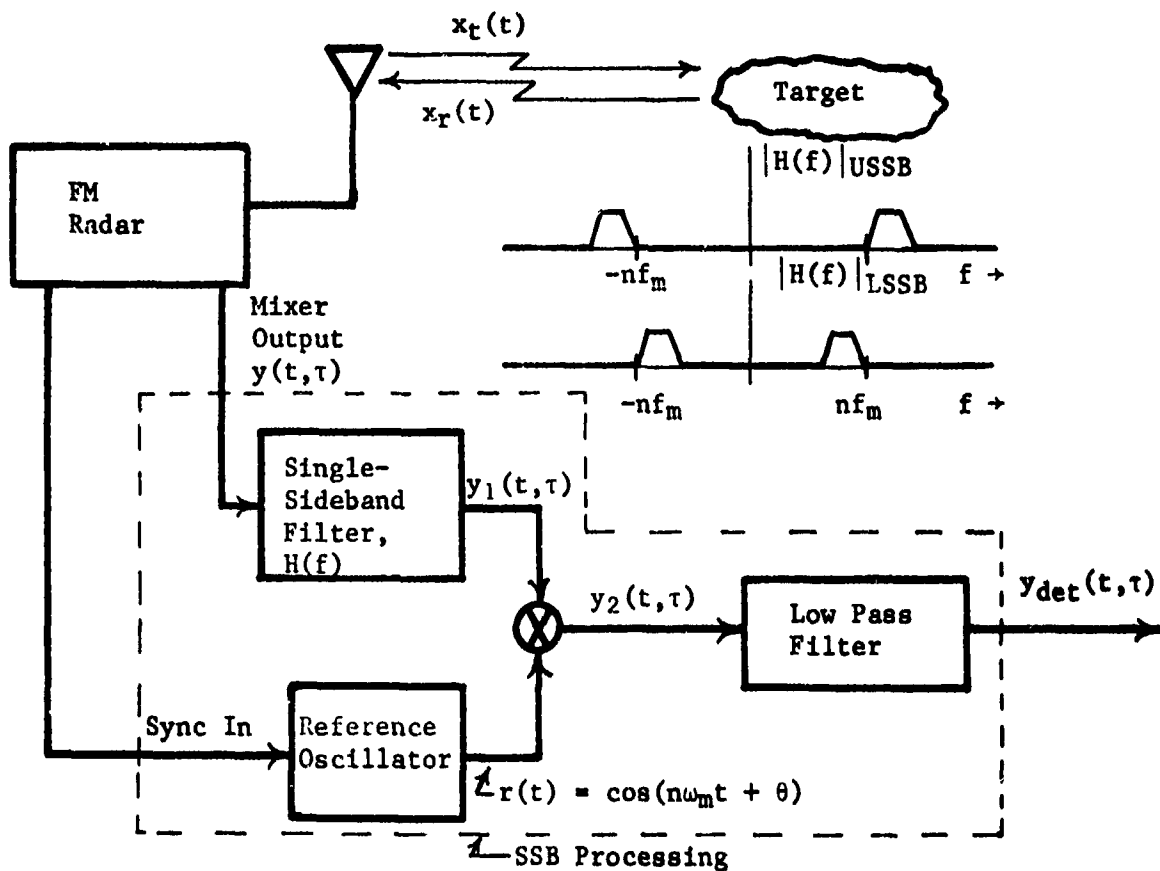
Figure 3. FM Radar With SSB Harmonic Processing*

The multiplier output is

$$y_2(t,\tau) = y_1(t,\tau)r(t)$$

$$= y_1(t,\tau)\mathrm{Re}\{e^{j(n\omega_m t+\theta)}\}$$

Using the identity $v_1 v_2 = \tfrac{1}{2}\mathrm{Re}\{z_1 z_2^*\} + \tfrac{1}{2}\mathrm{Re}\{z_1 z_2\}$ when $v_1 \triangleq \mathrm{Re}\{z_1\}$ and $v_2 \triangleq \mathrm{Re}\{z_2\}$ and assuming that $n \neq 0$, the detector output is

$$y_{det}(t,\tau) = \begin{bmatrix} \dfrac{1}{2}\,\mathrm{Re}\{c_{\pm n}e^{j(\pm n\omega_m+\omega_d)t}\,e^{\mp j(n\omega_m t+\theta)}\} & , & \omega_d > 0 \\[2em] \dfrac{1}{2}\,\mathrm{Re}\{c_{\mp n}^{-}e^{j(\mp n\omega_m+\omega_d)t}\,e^{\pm j(n\omega_m t+\theta)}\} & , & \omega_d < 0 \end{bmatrix}$$

$$= \begin{bmatrix} \dfrac{1}{2}\,\mathrm{Re}\{c_{\pm n}(\tau)e^{j(\omega_d t\mp\theta)}\} & , & \omega_d > 0 \\[2em] \dfrac{1}{2}\,\mathrm{Re}\{c_{\mp n}^{-}(\tau)e^{j(\omega_d t\pm\theta)}\} & , & \omega_d < 0 \end{bmatrix} \quad .$$

---

*The SSB processor shown here is the filter type. Assuming ideal filters, the same result is obtained if the phasing type—also known as Kalmus filter [5,12,13]— is used.

17

Thus, the detector (doppler) output is

$$y_{det}(t,\tau) = \left[\begin{array}{l} \frac{1}{2}|c_{\pm n}(\tau)| \ \cos \ [\omega_d t \mp \theta + \underline{/c_{\pm n}(\tau)}] \quad , \quad \omega_d > 0 \\[2em] \frac{1}{2}|c_{\mp n}(\tau)| \ \cos \ [\omega_d t \pm \theta + \underline{/c_{\mp n}(\tau)}] \quad , \quad \omega_d < 0 \end{array}\right] \tag{40}$$

The range law for the SSB detector is

$$R_n(\tau) = \left[\begin{array}{l} \frac{1}{2}|c_{\pm n}(\tau)| \quad , \quad \omega_d > 0 \\[2em] \frac{1}{2}|c_{\mp n}(\tau)| \quad , \quad \omega_d < 0 \end{array}\right] \tag{41}$$

where the upper signs give the response if an USSB filter is used in the processor and the lower signs give the response for an LSSB filter.

For detection of directional doppler we require a modulating waveshape such that the $|c_{+n}(\tau)|$ is appreciably different from the $|c_{-n}(\tau)|$ for the range of τ that is of interest (usually $\tau > 0$). If an USSB filter is used in the processor, $|c_{+n}(\tau)|$ is obtained for positive doppler frequencies (receding targets) and $|c_{-n}(\tau)|$ for approaching targets. Conversely, an LSSB doppler filter would be used to obtain $|c_{+n}(\tau)|$ for approaching targets and $|c_{-n}(\tau)|$ for receding targets. For example, if a positive-slope sawtooth modulating waveform is used, Figure 10 shows that $|c_{+n}(\tau)|$ peaks up at $x = 2B\tau \approx n$ and $|c_{-n}(\tau)|$ peaks up at $x = -2B\tau \approx -n$ and it is approximately zero for positive τ.

6. FOURIER COEFFICIENTS FOR A PIECEWISE LINEAR MODULATING WAVEFORM

As seen from the above, the complex Fourier coefficients $\{c_k\}$ must be known in order to determine the range law. These coefficients are difficult to obtain for frequency modulation by a complicated waveshape but, by approximating the modulating voltage with a series of straight lines, a general formula for the $\{c_k\}$ may be obtained.

Referring to Figure 4, any periodic modulating waveform may be specified as precisely as desired by using a sufficient number of piecewise-linear segments. $f_i(t)$ is the instantaneous frequency of the FM radar with respect to the carrier frequency and B is the peak-to-peak frequency deviation. $\{\psi_\ell\}$ and $\{\rho_\ell\}$ are the parameters that specify the fractional frequency excursion and fractional time duration of the ℓth linear segment.

$x = 2B\tau$

τ = round-trip time delay

B = p-p frequency deviation

$\rho_1 + \rho_2 + \rho_3 + \rho_4 \equiv 1$

where ρ_ℓ = "duty-cycle" during ℓth interval

ψ_ℓ = frequency deviation over the ℓth interval
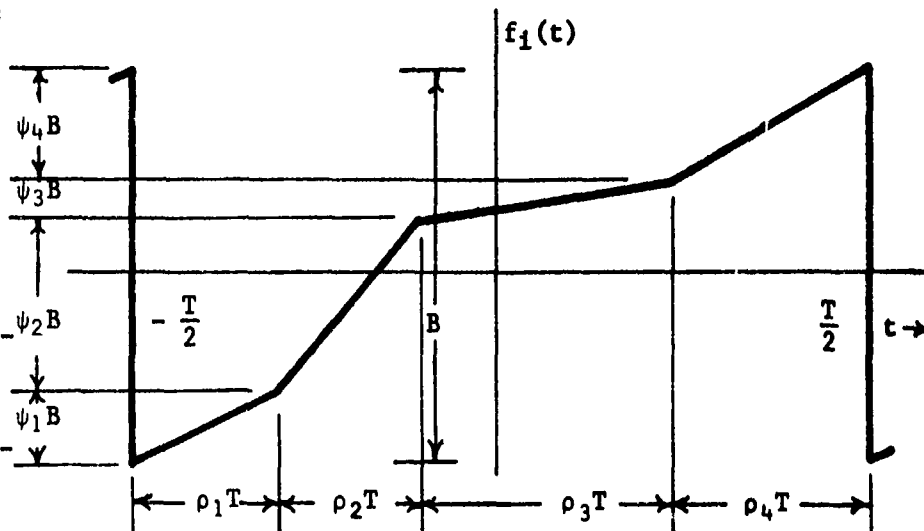
<u>Note</u> ψ_ℓ may be negative.

Figure 4. Piecewise Linear Modulating Waveform for L=4 Segments

6.1 General Case

Referring to (8) the Fourier coefficients are given by

$$c_k = \frac{1}{T} \int_{-T/2}^{T/2} e^{j\theta_d(t,\tau)} e^{jk\omega_m t} dt \qquad (42a)$$

where

$$\theta_d(t,\tau) = 2\pi \int_{t-\tau}^{t} f_i(t)dt \qquad (42b)$$

Referring to Figure 5, the instantaneous frequency during the ℓth interval is

$$f_i(t) = \left[\frac{\psi_\ell B}{\rho_\ell T} (t-t_\ell) + f_\ell \quad , \quad \ell\text{th interval} \right] \qquad (43)$$
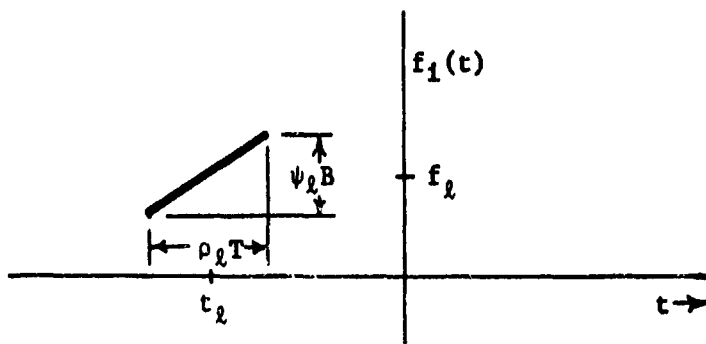
Figure 5. Piecewise-Linear Segment

Substituting (43) into (42b) the difference phase during the ℓth interval, where τ is assumed to be small with respect to $\rho_\ell T$ so that the exact behavior of $\theta_d(t)$ during the turn-around time can be neglected, is

$$\theta_d(t,\tau) = [\omega_\ell t + \theta_\ell] \quad , \quad \ell\text{th interval} \tag{44}$$

where $\omega_\ell = \dfrac{\omega_k}{\rho_k}\dfrac{\pi}{T} x =$ difference frequency during the ℓth interval $\qquad$ (45)

$$\theta_\ell \overset{\Delta}{=} \pi \left[\beta_\ell - \frac{\psi_\ell}{\rho_\ell}\alpha_\ell\right]x = \text{phase constant during the } \ell\text{th interval} \tag{46}$$

$$x \overset{\Delta}{=} 2B\tau \tag{47}$$

$$\alpha_\ell \overset{\Delta}{=} \frac{1}{T}t_\ell = -\frac{1}{2}\left[1 - 2\left(\sum_{j=1}^{\ell-1}\rho_j\right) - \rho_\ell\right] \tag{48}$$

$$\beta_\ell \overset{\Delta}{=} \frac{1}{B}f_\ell = -\frac{1}{2}\left[1 - 2\left(\sum_{j=1}^{\ell-1}\psi_j\right) - \psi_\ell\right] \tag{49}$$

Substituting (44) into (41), it becomes

$$c_k = \frac{1}{T}\sum_{\ell=1}^{L}\left[\int_{\ell\text{th interval}} e^{j[\omega_\ell t + \theta_\ell]} e^{jk\omega_m t}dt\right] \tag{50}$$

where L is the number of segments that are used over a period of the modulation waveform. Equation (50), when evaluated, becomes

$$c_k(\tau) = \sum_{\ell=1}^{L}\left[\rho_\ell \, e^{j\pi\{[\beta_\ell - \frac{\psi_\ell}{\rho_\ell}\alpha_\ell]x - [1-2(\sum_{j=1}^{\ell-1}\rho_j)-\rho_\ell](\frac{\psi_\ell}{2\rho_\ell}x-k)\}}\right.$$
$$\left. \cdot \; \frac{\sin\left[\frac{\pi}{2}(\psi_\ell x - 2\rho_\ell k)\right]}{\frac{\pi}{2}(\psi_\ell x - 2\rho_\ell k)}\right] \cdot$$

Using (48) and (49) this can be reduced to

$$c_k(\tau) = \sum_{\ell=1}^{L}\rho_\ell e^{+j\phi_\ell(x)}\;\frac{\sin\left[\frac{\pi}{2}(\psi_\ell x - 2\rho_\ell k)\right]}{\frac{\pi}{2}(\psi_\ell x - 2\rho_\ell k)} \tag{51}$$

where

$$\phi_\ell(x) = +\frac{\pi}{2}\{[1-2(\sum_{j=1}^{\ell-1}\rho_j)-\rho_\ell]2k - [1-2(\sum_{j=1}^{\ell-1}\psi_j)-\psi_\ell]x\} \tag{52}$$

L is the total number of piecewise-linear segments

ρ_ℓ is the proportional part of the period that is used by the ℓth linear segment

ψ_ℓ is the proportional part of the peak-to-peak frequency deviation used by the ℓth linear segment

$x = 2B\tau$ is the normalized round-trip time delay to the target where τ is the actual time delay and B is the peak-to-peak frequency deviation.

In using this equation, note that $\displaystyle\sum_{j=1}^{\ell-1} \rho_j \equiv 0$ for $\ell = 1$.

The $\{c_k\}$ of (51) can be evaluated by use of a digital computer. The $\{c_k\}$ approximate the $\{c_k\}$ of any modulating signal waveshape since the piecewise linear waveform can approximate any modulating waveshape as accurately as desired by taking enough segments.

> The range response corresponding to any modulation waveshape can then be evaluated for incoherent processing by use of (51) in (21); or for coherent harmonic processing with a periodic reference by using (51) in (29) and (31).

In summary, once (51), (21), (29) and (31) are programed on a digital computer, the range response of any FM radar with harmonic processing can be obtained by simply specifying the parameters of the piecewise-linear modulating waveform. Equation (51) can also be used to obtain simplified solutions when L is not too large.

The accuracy of the range law obtained from the piecewise-linear approximation is shown in Appendix I.

6.2 Example 1--Non-Symmetrical Triangular FM

The Fourier coefficients $\{c_k\}$ will now be evaluated for a non-symmetrical triangular waveform as shown in Figure 6.
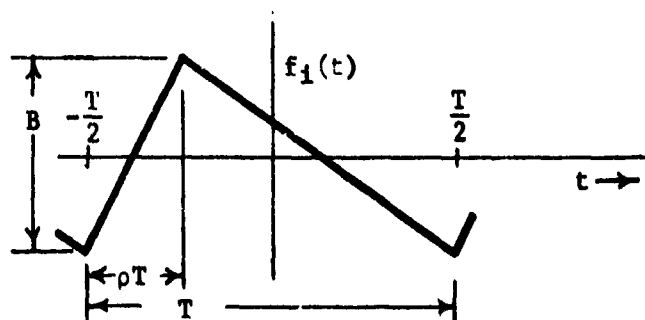
Figure 6. Non-Symmetrical Triangular Modulation

Comparing Figure 6 with Figures 4 and 5 it is seen that

$$L = 2$$
$$\rho_1 = \rho \;,\; \rho_2 = 1-\rho$$
$$\psi_1 = 1 \;,\; \psi_2 = -1$$

21

Using these parameters in (51), the Fourier coefficients for $v(t)^*v(t-\tau)$ corresponding to a non-symmetrical triangular modulating waveform are then

$$c_k = \rho e^{j\pi(1-\rho)k} \frac{\sin\left[\frac{\pi}{2}(x-2\rho k)\right]}{\frac{\pi}{2}(x-2\rho k)}$$

$$+ (1-\rho)e^{-j\pi\rho k} \frac{\sin\left[\frac{\pi}{2}(x+2(1-\rho)k)\right]}{\frac{\pi}{2}(x+2(1-\rho)k)} \qquad (53)$$

where ρ is the "duty cycle" of the up-sweep of the non-symmetrical triangle waveform.

6.3 Example 2--Symmetrical Triangular FM

When the triangle modulation is symmetric, $\rho = \frac{1}{2}$ and (53) reduces to the well-known coefficients [5,6,9]:

$$c_k = \frac{1}{2} e^{j\frac{\pi}{2}k} \left[\frac{\sin\frac{\pi}{2}(x-k)}{\frac{\pi}{2}(x-k)} + (-1)^k \frac{\sin\frac{\pi}{2}(x+k)}{\frac{\pi}{2}(x+k)} \right] \qquad (54)$$

6.4 Example 3--Stepped Triangle FM

A stepped-triangle FM waveform is shown in Figure 7 below. Using (51) with
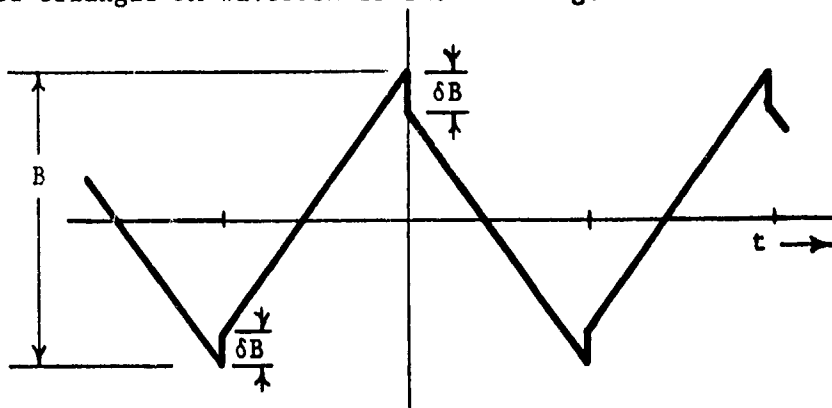
Figure 7. Stepped-Triangle FM

L=4, the Fourier coefficients are

$$c_k = \frac{1}{2} e^{j\frac{\pi}{2}(\delta x+k)} \frac{\sin\frac{\pi}{2}[(1-\delta)x-k]}{\frac{\pi}{2}[(1-\delta)x-k]} + \frac{1}{2} e^{-j\frac{\pi}{2}(\delta x+k)} \frac{\sin\frac{\pi}{2}[(1-\delta)x+k]}{\frac{\pi}{2}[(1-\delta)x+k]} \qquad (55)$$

Using coherent detection with a sinusoidal reference, $r(t) = \cos[n\omega_m t + \theta]$, the resulting range response is, from (35) and (36)

$$R_n(\tau) = |z_n| \qquad (56)$$

where

$$z_n = \frac{1}{2}e^{j\frac{\pi}{2}n}\left[\cos(\frac{\pi}{2}\delta x - \theta)\ \frac{\sin\frac{\pi}{2}[(1-\delta)x-n]}{\frac{\pi}{2}[(1-\delta)x-n]} + (-1)^n\cos(\frac{\pi}{2}\delta x + \theta)\ \frac{\sin\frac{\pi}{2}[(1-\delta)x+n]}{\frac{\pi}{2}[(1-\delta)x+n]}\right] \qquad (57)$$

The graph of this range response will be discussed below. These examples show how the complexity of (51) can be reduced for some particular waveshapes. However, (51) is the general equation for the $\{c_k\}$ to be used in (28) and (29).

7. COMPUTED RANGE LAWS

7.1 Linear Modulation and Coherent Detection with a Sinusoidal Reference

As an example of the synthesis of a range law by using (51) to obtain the c_n to be used in (35) and (36), we will choose the fourth harmonic law (n=4) and a sine-wave reference (at a phase angle θ_r) so that the relative range law is determined from

$$|z_4(\tau)| = |c_{-4}(\tau)e^{j\theta_r} + c_4(\tau)e^{-j\theta_r}| \qquad (58)$$

The modulating waveform and the reference voltage are then related as shown below
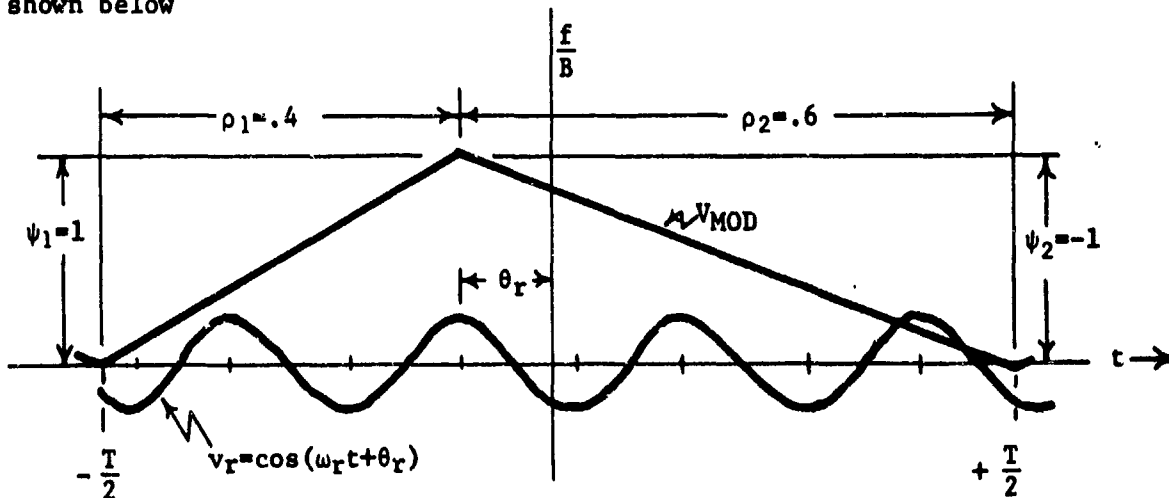
The results of computing the values of $c_{\pm 4}$ are given on Figure 8, where the amplitude and phase of each c are shown. Since the detection angle is $0°$, c_4 and c_{-4} are added vectorially to obtain the range law r_4 and its associated doppler phase $\underline{/z_4}$.

As was pointed out by (12), the two c's involved are the values of the (complex) ambiguity function evaluated along the $\pm 4\omega_m$ axes. By single-sideband detection techniques, either c_4 or c_{-4} can be detected separately or they may be combined according to (58) by detecting with a coherent sine-wave reference at an angle of θ_r. The result of changing the reference phase from 0 to 0.4π is shown on Figure 9. The range response is now a more acceptable single-lobe response of larger amplitude and lower side-lobe level.

Figures 10, 11, and 12 show examples of standard linear sweep FM. The saw-tooth sweeps of Figures 10 and 11 exhibit unsymmetrical sideband responses whereas the triangular sweep of Figure 12 exhibits symmetrical sideband responses.

7.2 Non-Linear Modulation--N=0 Range Law

A simple example of non-linear FM modulation is obtained by the addition of a square wave to linear sweep. Figure 13 shows an example of the n=0 range law for this type of modulation. In this example the normal sin U/U range law is modified to, using (57) in (35) and (36)

$$R_0(x) = \frac{\sin \left[\frac{\pi}{2}(1-\delta)x\right]}{\left[\frac{\pi}{2}(1-\delta)x\right]} \cos \left[\frac{\pi}{2} \delta x\right] \quad , \quad x = 2B\tau \tag{59}$$

The first null of the cosine term can be positioned to cancel the peak of the first range sidelobe to produce a lower side-lobe level.

Adding a second square wave to the triangular FM can further reduce the side-lobes as shown on Figure 14. The range law is now given by:

$$R_0(\tau) = \frac{\sin \left[\frac{\pi}{2}(1-\delta_1-\delta_2)x\right]}{\left[\frac{\pi}{2}(1-\delta_1-\delta_2)x\right]} \cos \left[\frac{\pi}{2} \delta_1 x\right] \cos \left[\frac{\pi}{2} \delta_2 x\right] . \tag{60}$$

The maximum side-lobe ratio is now reduced to -27dB at the expense of widening the main lobe width from x=2 to x = 3.1 (a natural consequence of the law of conservation of volume under the ambiguity function). The extra nulls in the first two side-lobes are indicated by arrows and occur at $x_1 = 1/\delta_1$ and $x_2 = 1/\delta_2$.

The cosine modifiers shown in (60) apply not only to linear FM but also to any periodic modulation waveform when the square-waves are properly added to the waveform. For instance, for sine-wave FM, (60) is valid if the function $\frac{\sin [\ ]}{[\ ]}$ is replaced by $J_0[\ ]$.

A non-linear modulating waveform, such as one Taylor weighted [2] for a reduced side-lobe ratio, is approximated by seven straight line segments as shown on Figure 15. The computed range law shows a side-lobe ratio of -28dB, and a main lobe increased in width from x = 2 to x = 3.4. This result is more easily achieved by the addition of two square waves as was shown on Figure 14.

7.3 Non-Linear Modulation--Detection with a Sinusoidal Reference

Sidelobe reduction can also be accomplished on harmonic reference systems. As shown on Figures 16 and 17, the third harmonic range laws for frequency modulation by either a triangular or sawtooth waveform when combined with a synchronized square wave are identical. This response is obtained with a coherent sine wave reference given by $\cos (3\omega_m t + \pi/2)$. It is interesting to note that extra-ange law nulls do not exist in either the upper or lower sideband of Figure 15 whereas, on Figure 16, they exist in both sidebands.

7.4 Non-Linear Modulation--Detection with a Square-Wave Reference

An example of a computed fourth-harmonic range law using a square-wave reference voltage is shown on Figure 18. Here, we not only reduce the side-lobes with the addition of a square-wave to the linear modulation, but also eliminate the twelveth harmonic range law by phasing the reference voltage to 60°. Another example of a range law obtained by using a square-wave reference voltage is shown on Figure 19. The side-lobes here are even further reduced by adding two square-waves to the triangular modulation voltage.

The advantage of using square-waves added to the modulation and also for the reference of the coherent detector is that they are simply obtained in digital circuitry.

8. EXPERIMENTAL RANGE LAWS

Examples of experimentally measured range laws are shown on Figures 20, 21, and 2^. These curves illustrate that improved sidelobe levels can be obtained in practice and are in general agreement with the computed responses previously shown.

9. CONCLUSIONS

A general formula (51) for obtaining the complex Fourier coefficients to be used in determining the range law for a piecewise linear periodic frequency modulation waveform has been shown to be of great value in computing the range response for a complicated modulation. The approximate range response corresponding to *any* periodic modulating waveshape can be obtained by simply specifying the piecewise-linear parameters for that waveshape. The amplitude and phase of the complex Fourier coefficients provide the range response and doppler phase for single-sideband detection of the n'th harmonic. The vector addition of these appropriate coefficients with proper complex weighting gives the doppler output for double sideband (coherent or incoherent) detection.

Suppression of range side-lobes by using synchronized square-waves properly added to the periodic modulation was demonstrated to be realized with simple digital circuitry. This method was shown to be just as effective as the use of a more complicated non-linear Taylor-weighted modulation waveform.
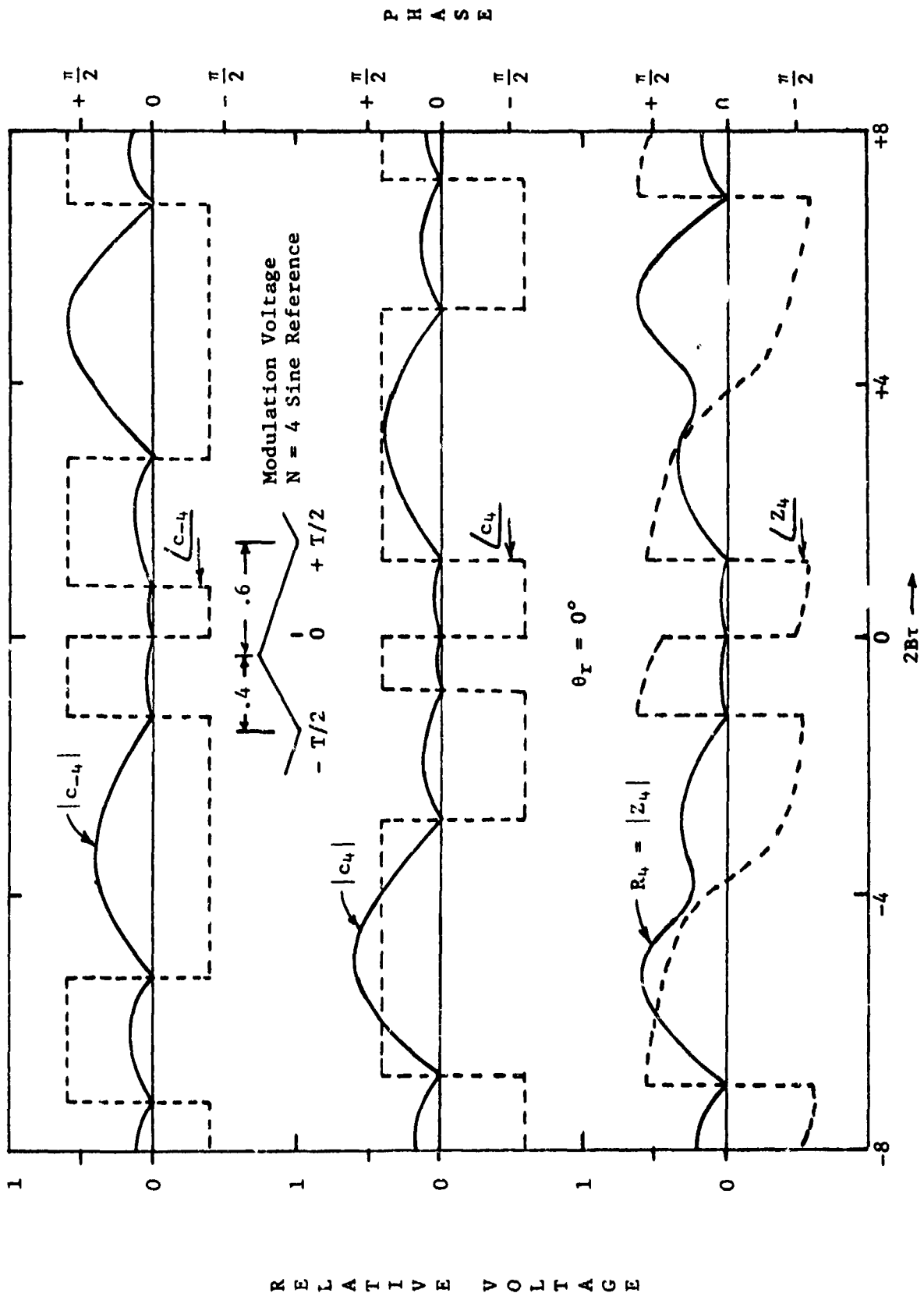
25

Figure 8. Fourth Harmonic Range Law For Unsymmetrical Triangular Modulation (Reference Voltage Phase Angle = 0)
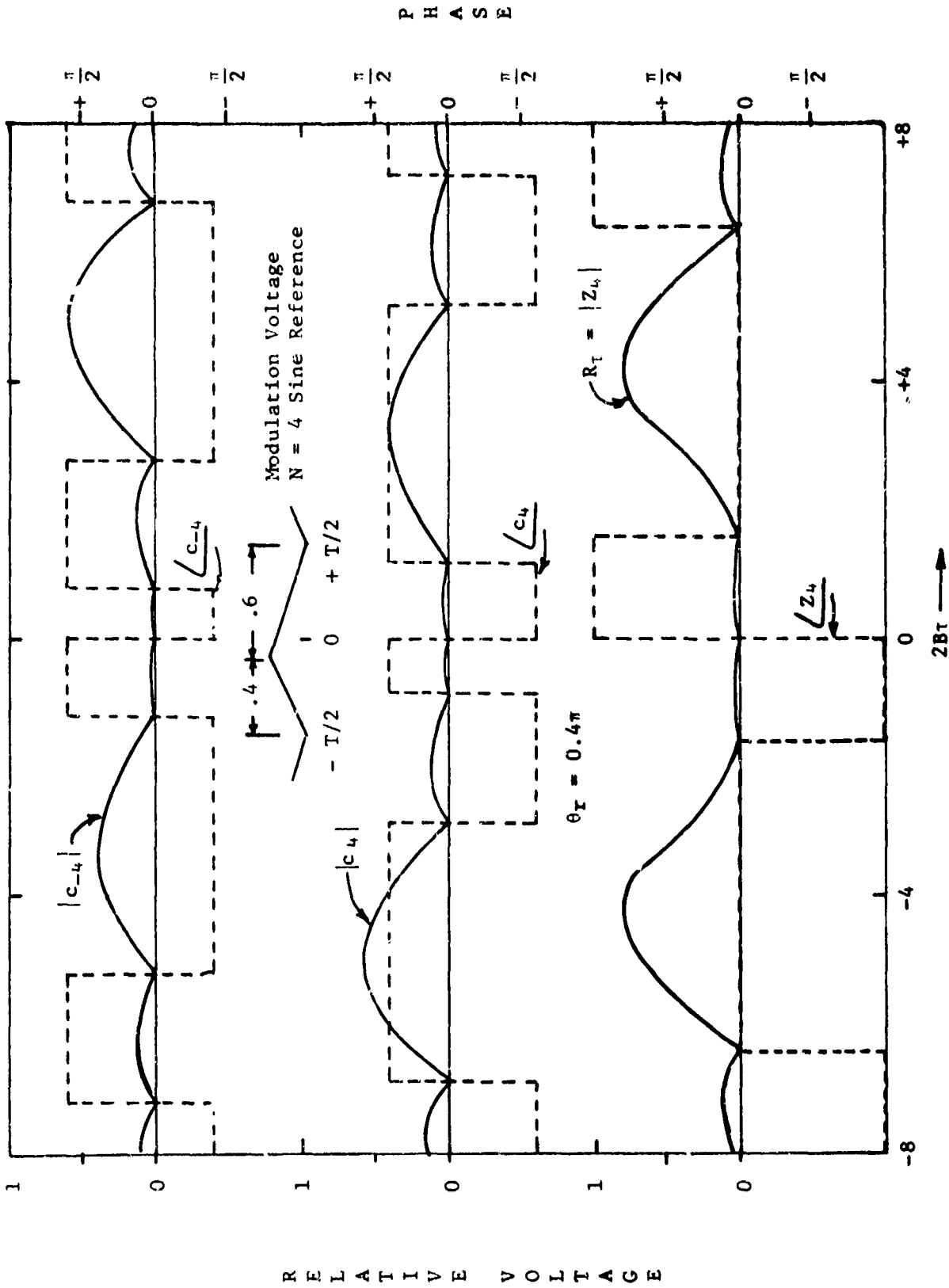
26

Figure 9. Fourth Harmonic Range Law For Unsymmetrical Triangular Modulation
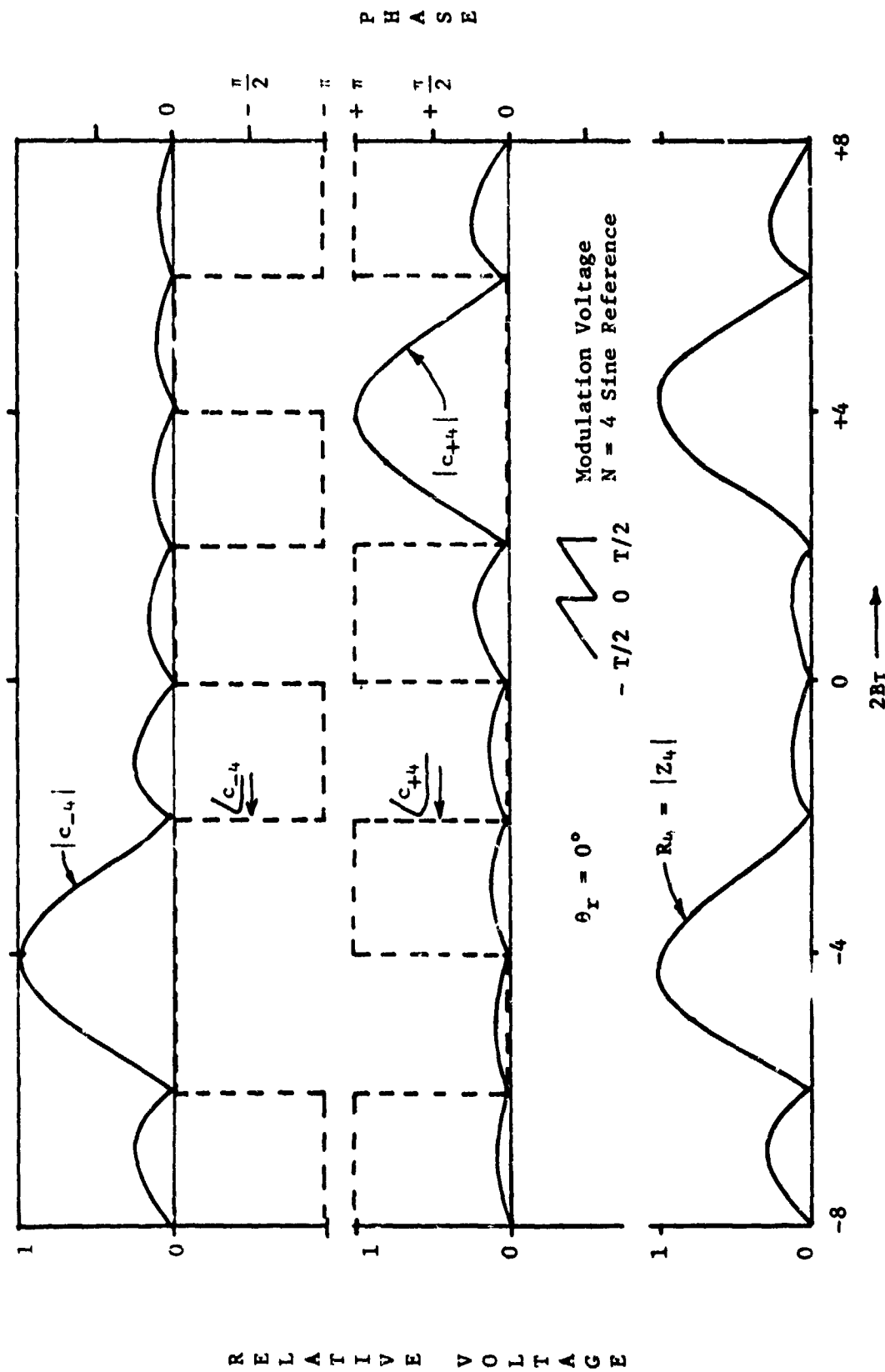(Reference Voltage Phase Angle = 0.4π)

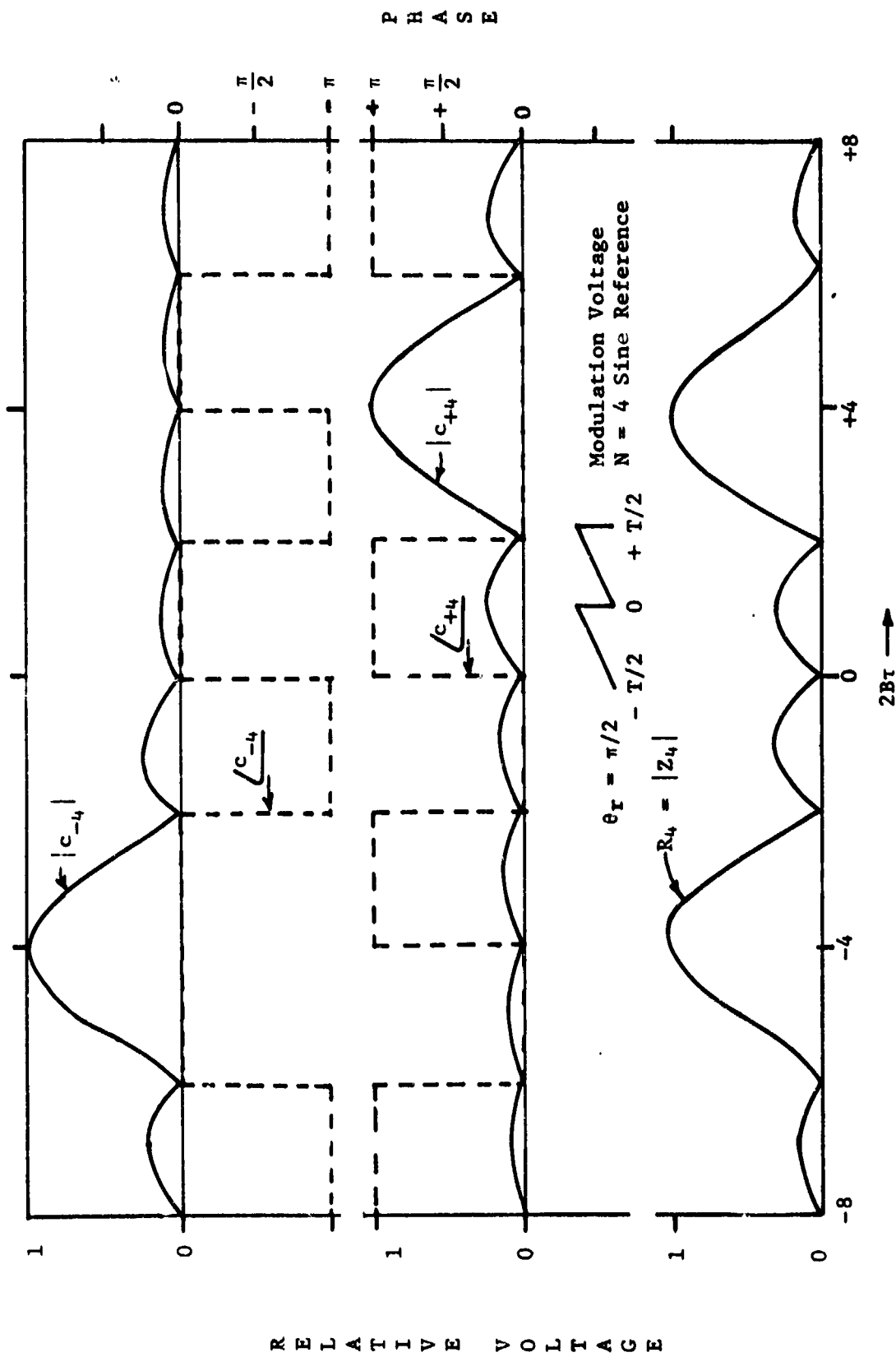Figure 10. Fourth Harmonic Range Law For Sawtooth Modulation ($\theta_r = 0$)

Figure 11. Fourth Harmonic Range Law For Sawtooth Modulation ($\theta_r = \pi/2$)
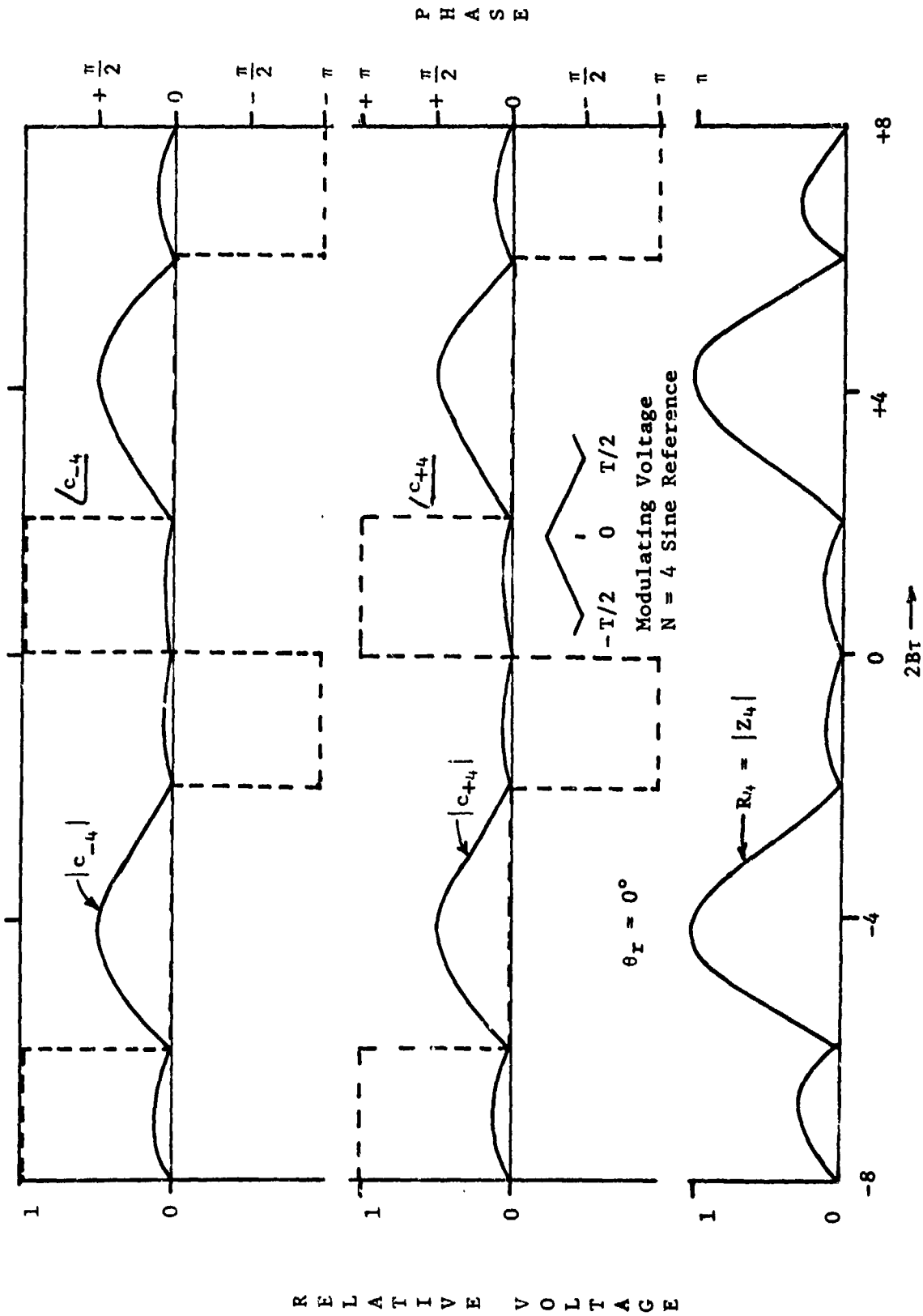
29

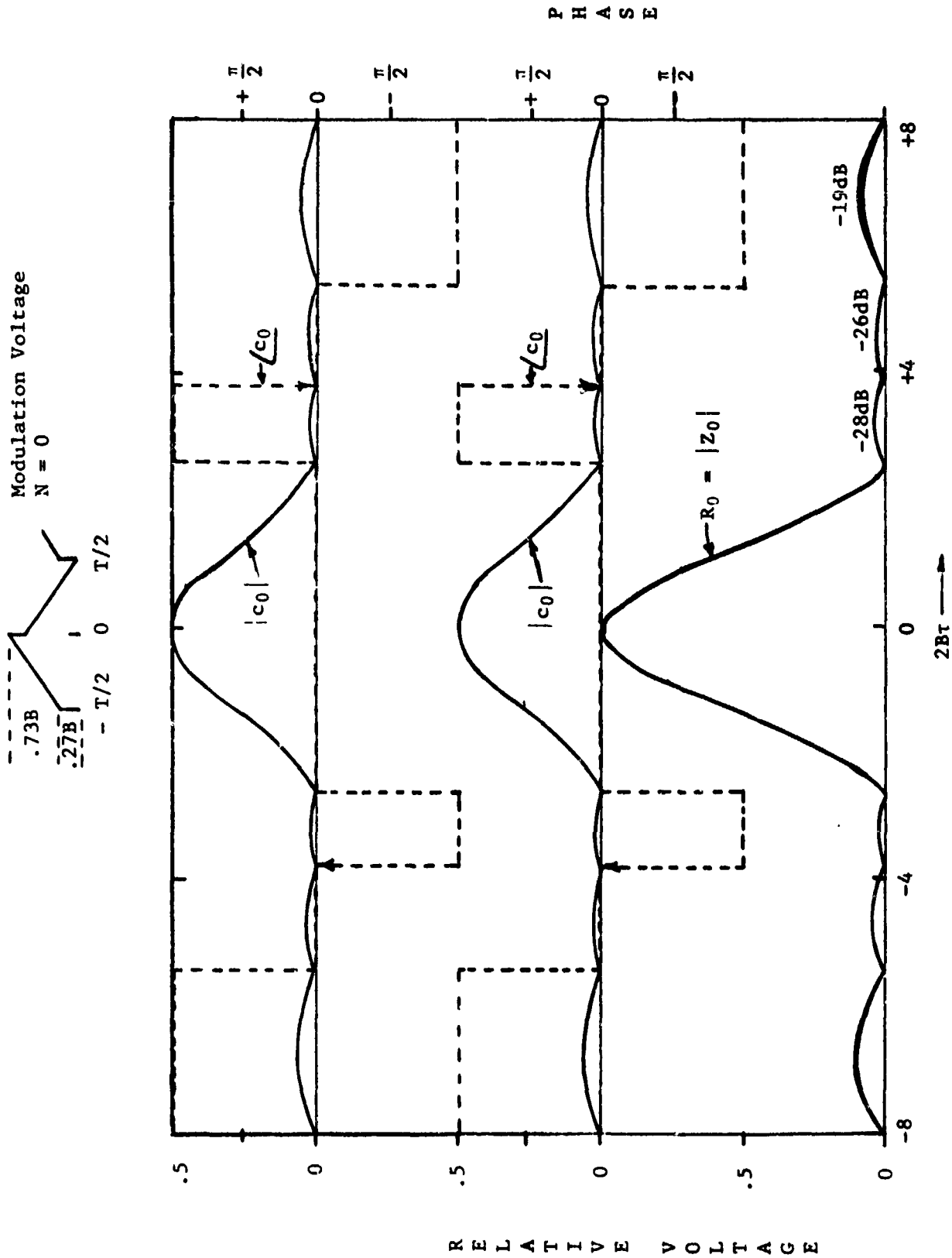Figure 12. Fourth Harmonic Range Law For Symmetrical Triangular Modulation

Figure 13. Zero Order Range Law For Triangle Plus Square Wave Modulation
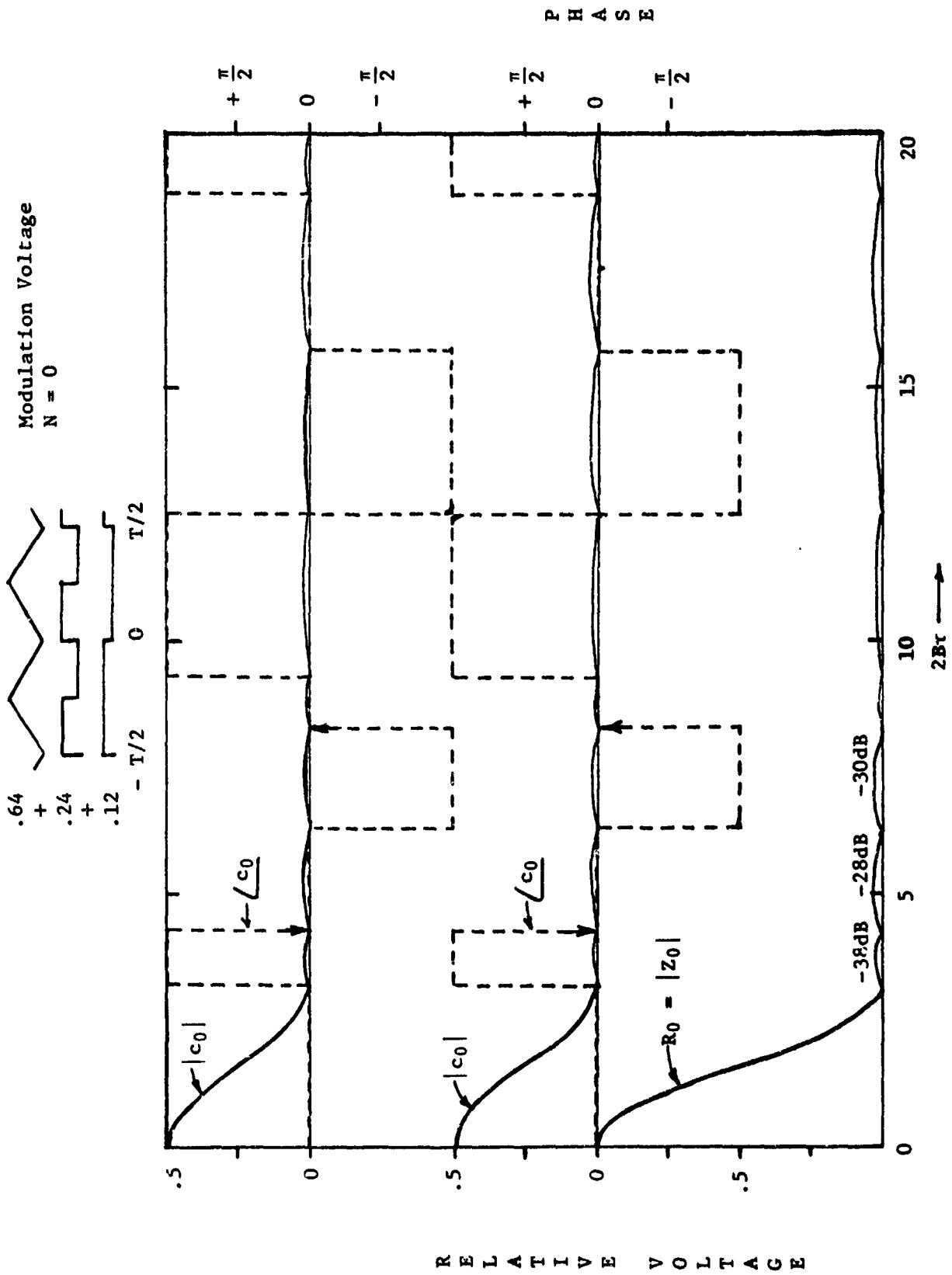
Figure 14. Zero Order Range Law For Triangle Plus Two Square Wave Modulation
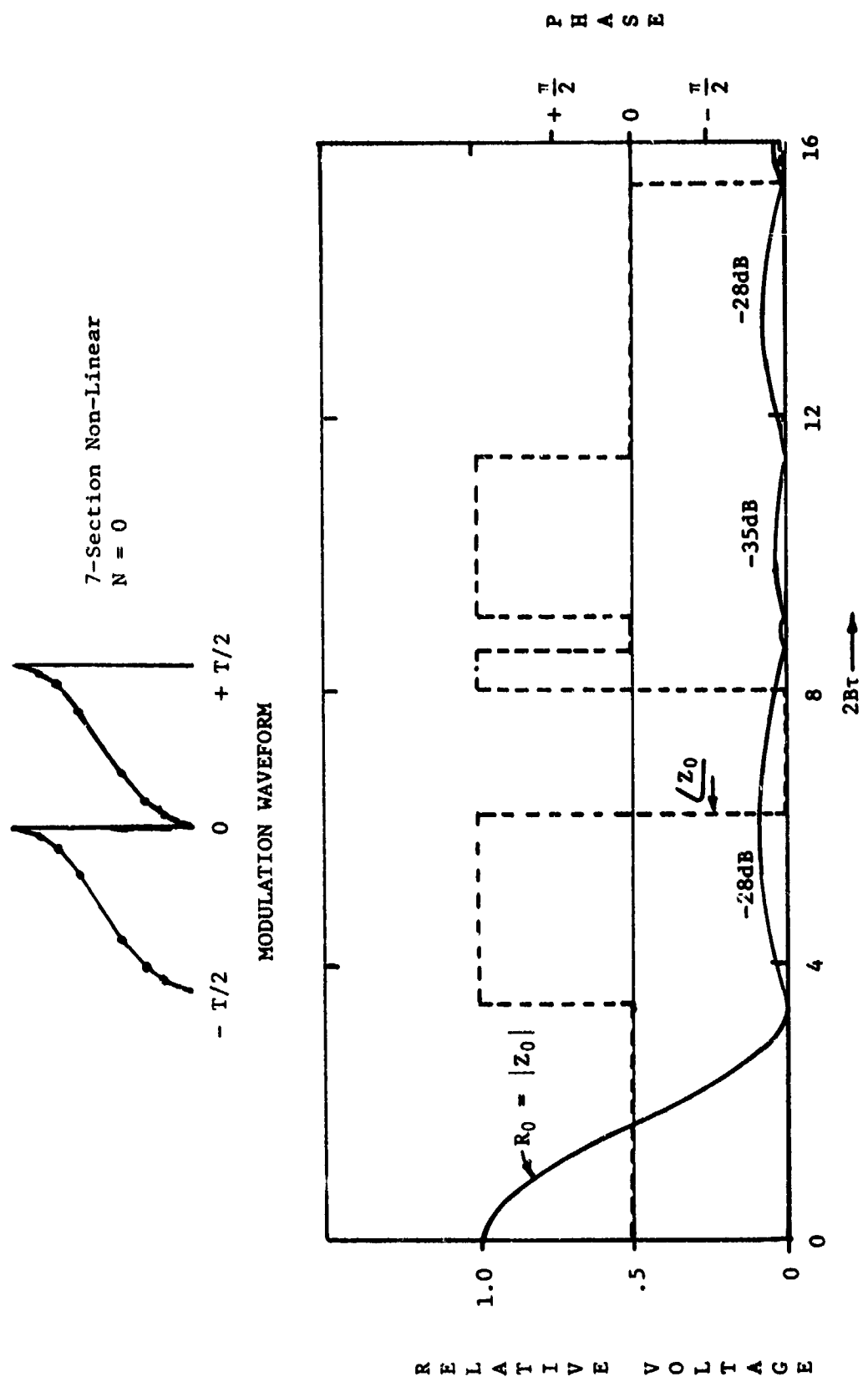
Figure 15. Zero Order Range Law For 7-Section Modulation Waveform
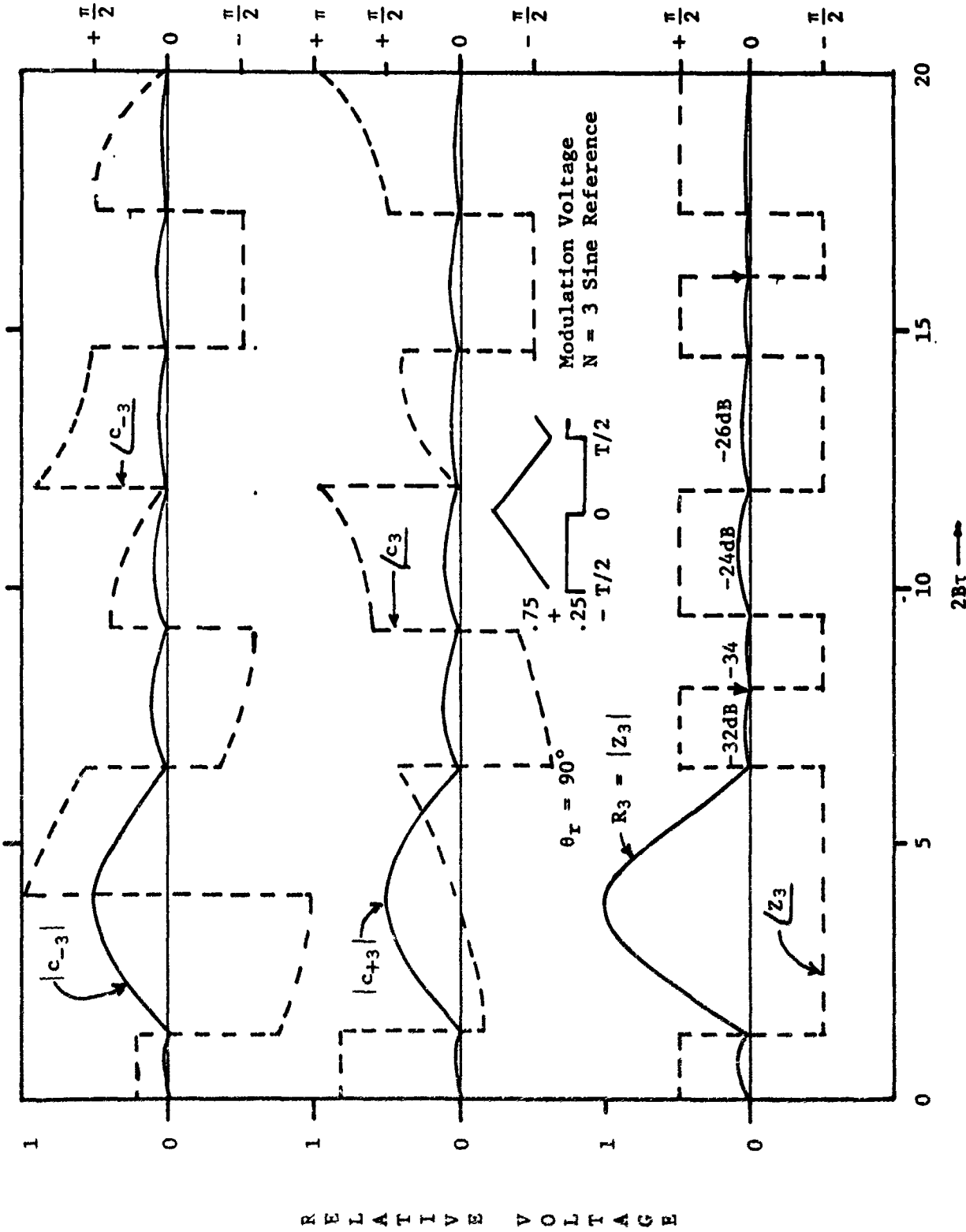
Figure 16. Third Harmonic Range Law For Triangle Plus Square Modulation
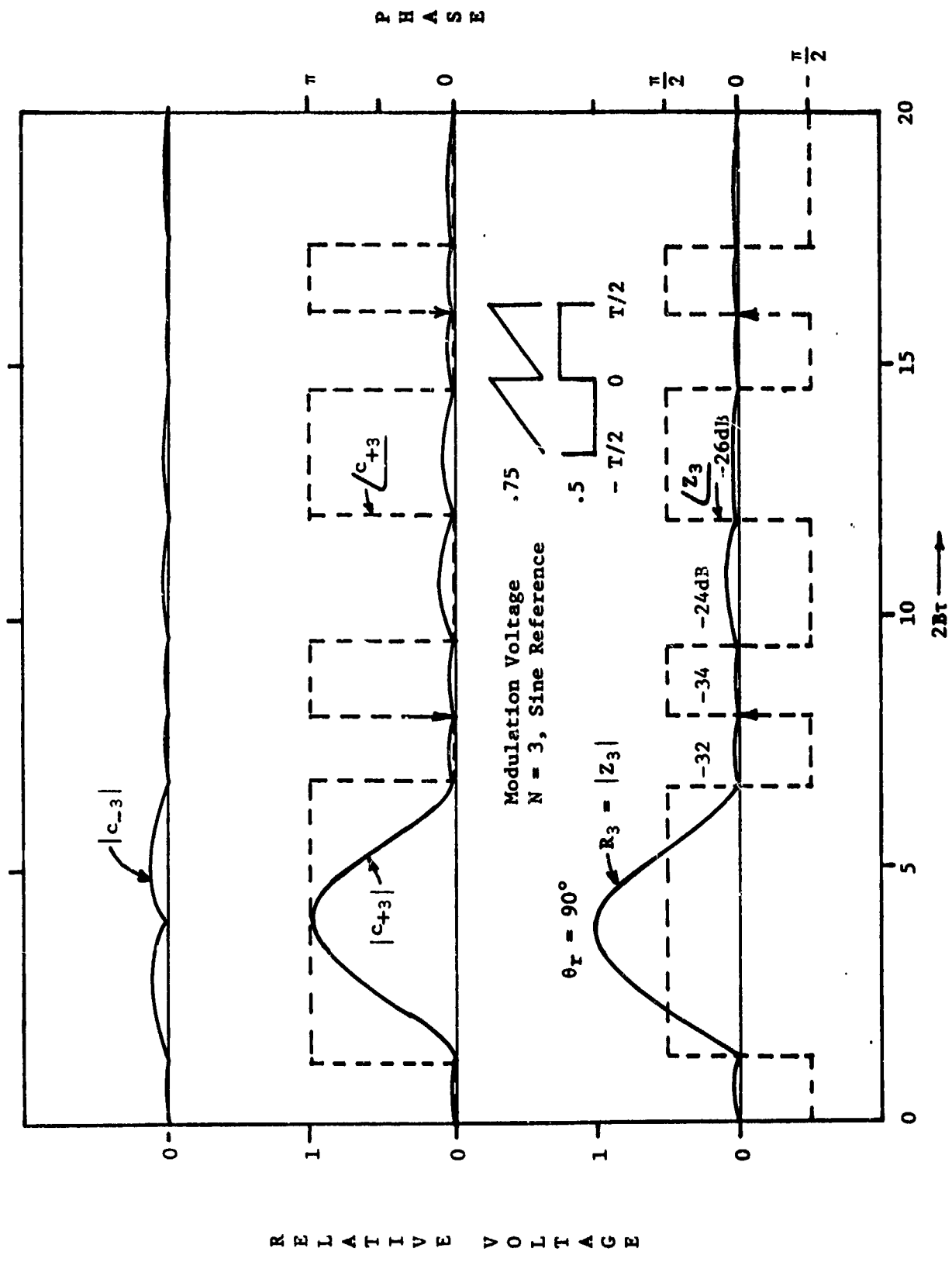
Figure 17. Third Harmonic Range Law For Sawtooth Plus Square Wave Modulation
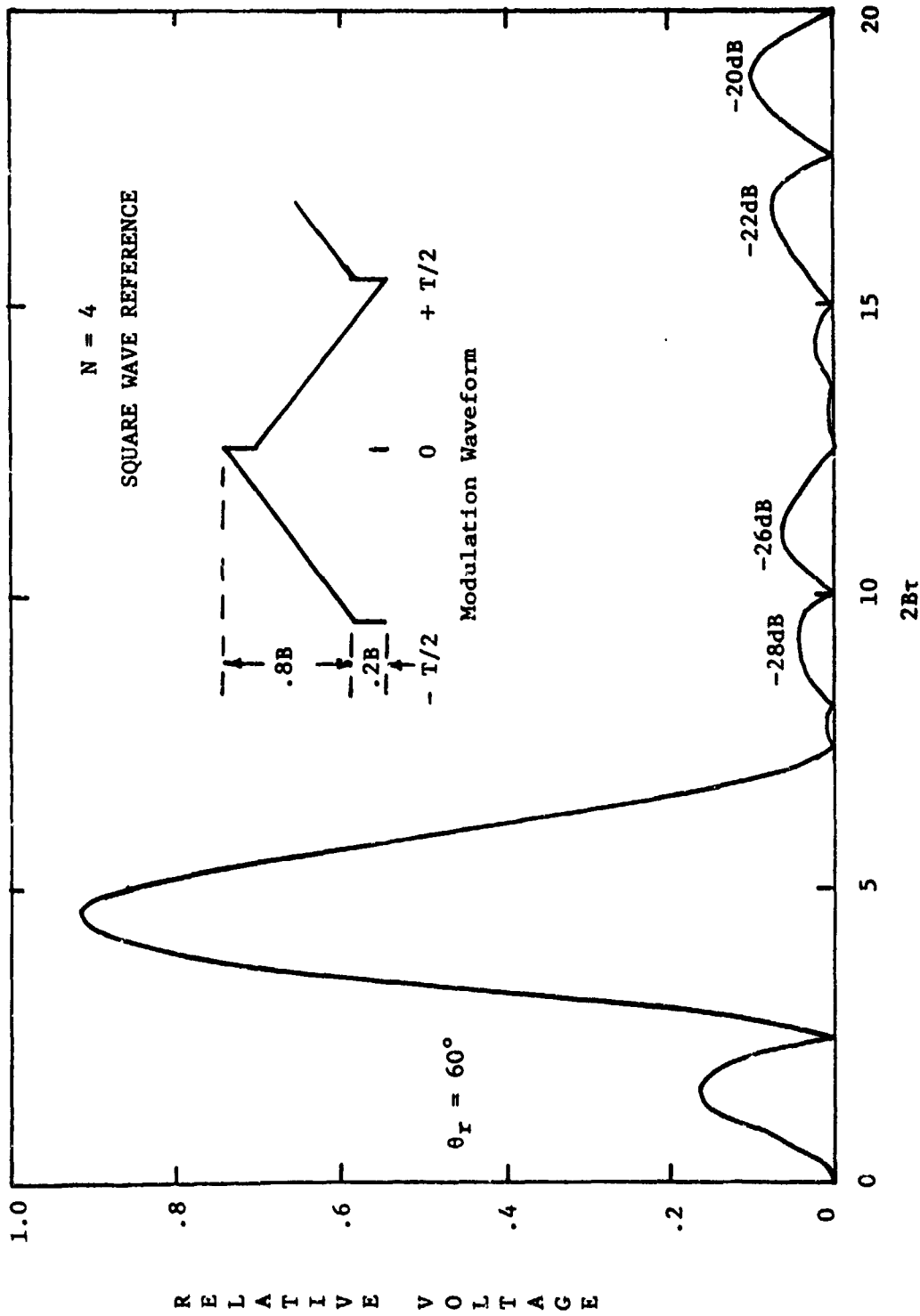
Figure 18. Fourth Harmonic Range Law Using Square Wave Reference
Waveform And Triangle Plus Square Wave Modulation
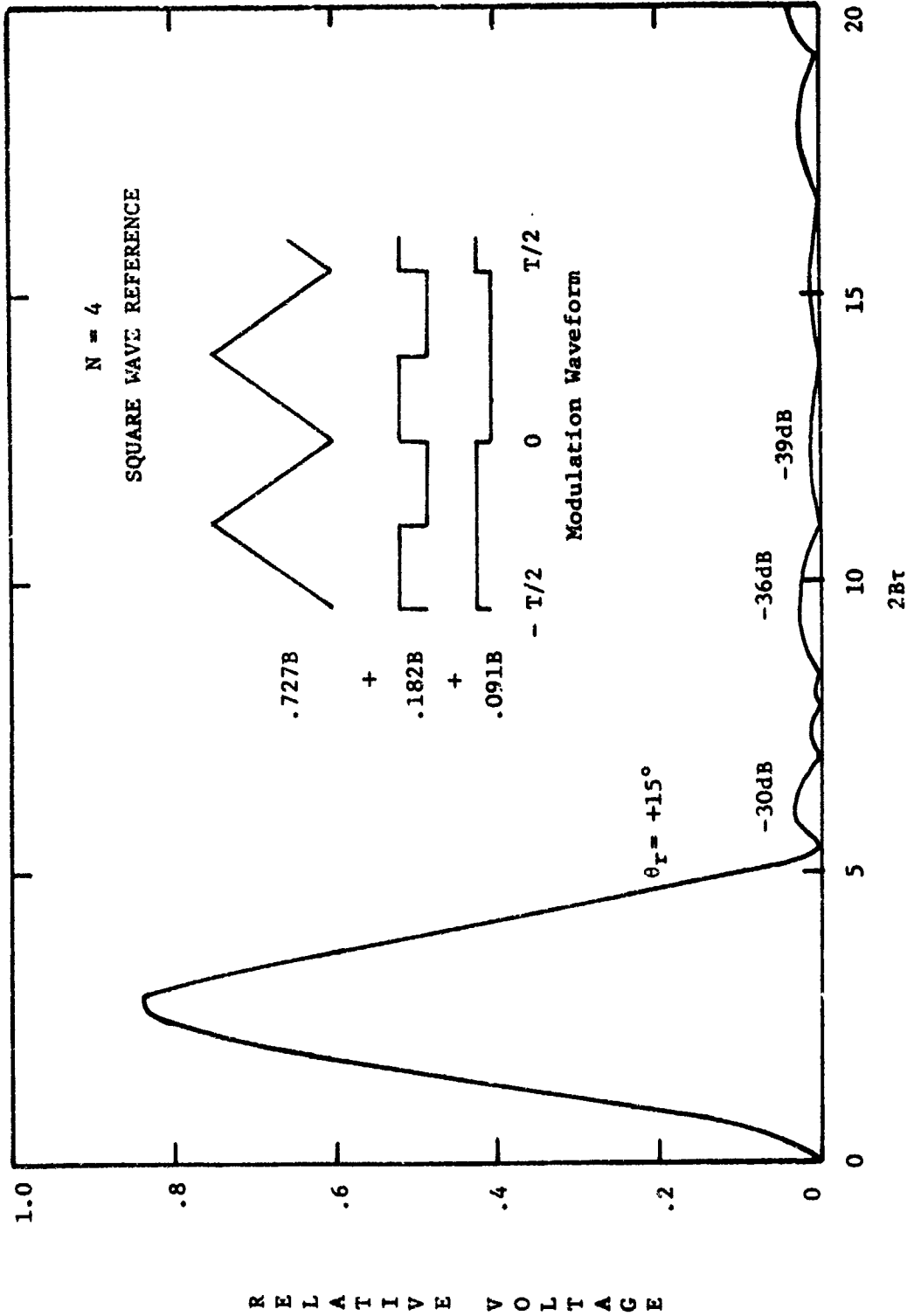
Figure 19. Fourth Harmonic Range Law Using Square Wave Reference
Waveform And Triangle Plus Two Square Wave Modulation
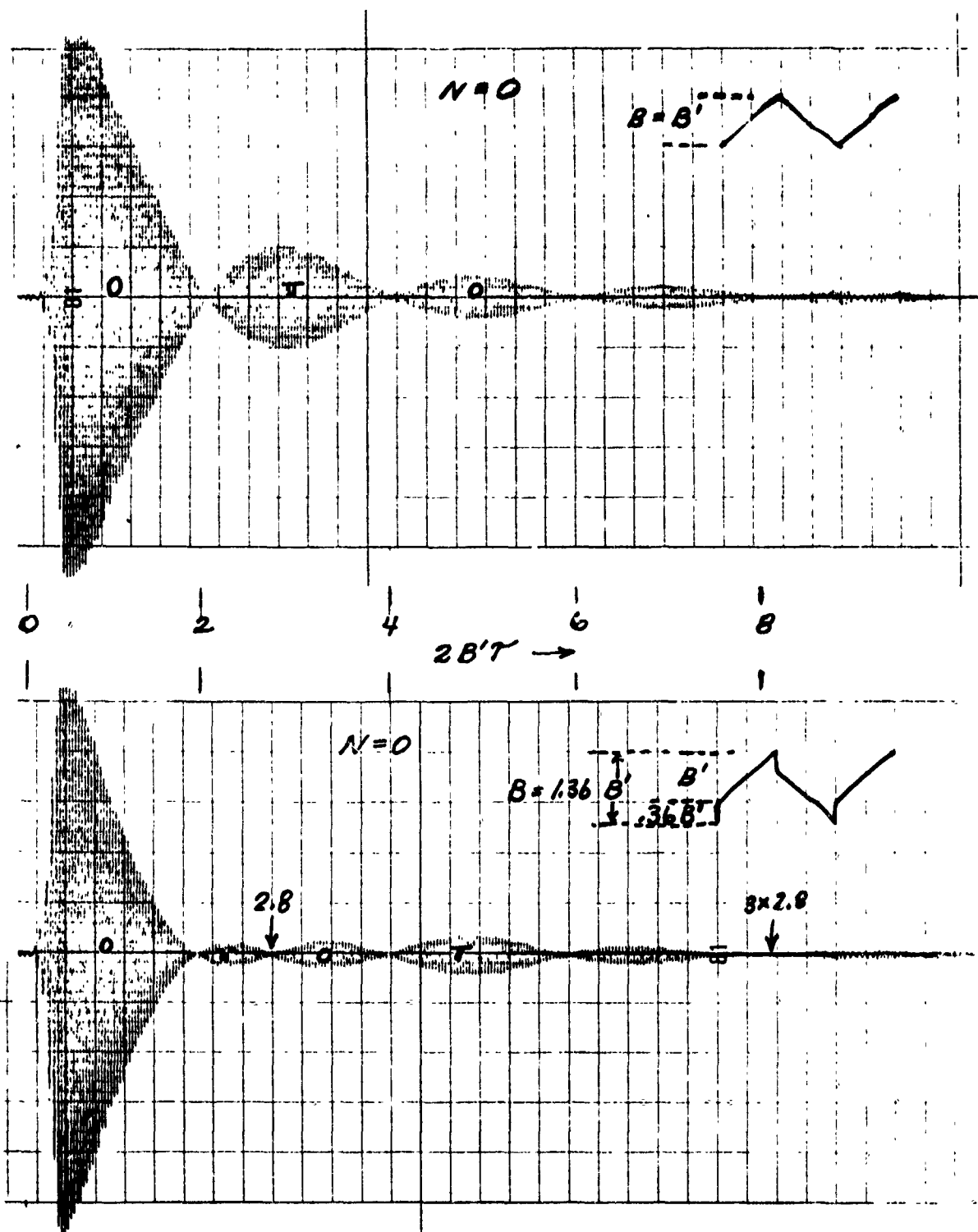
Figure 20. Effect of Square Wave Added to Modulation for N = 0
Range Law (Measured on Exponential Line)
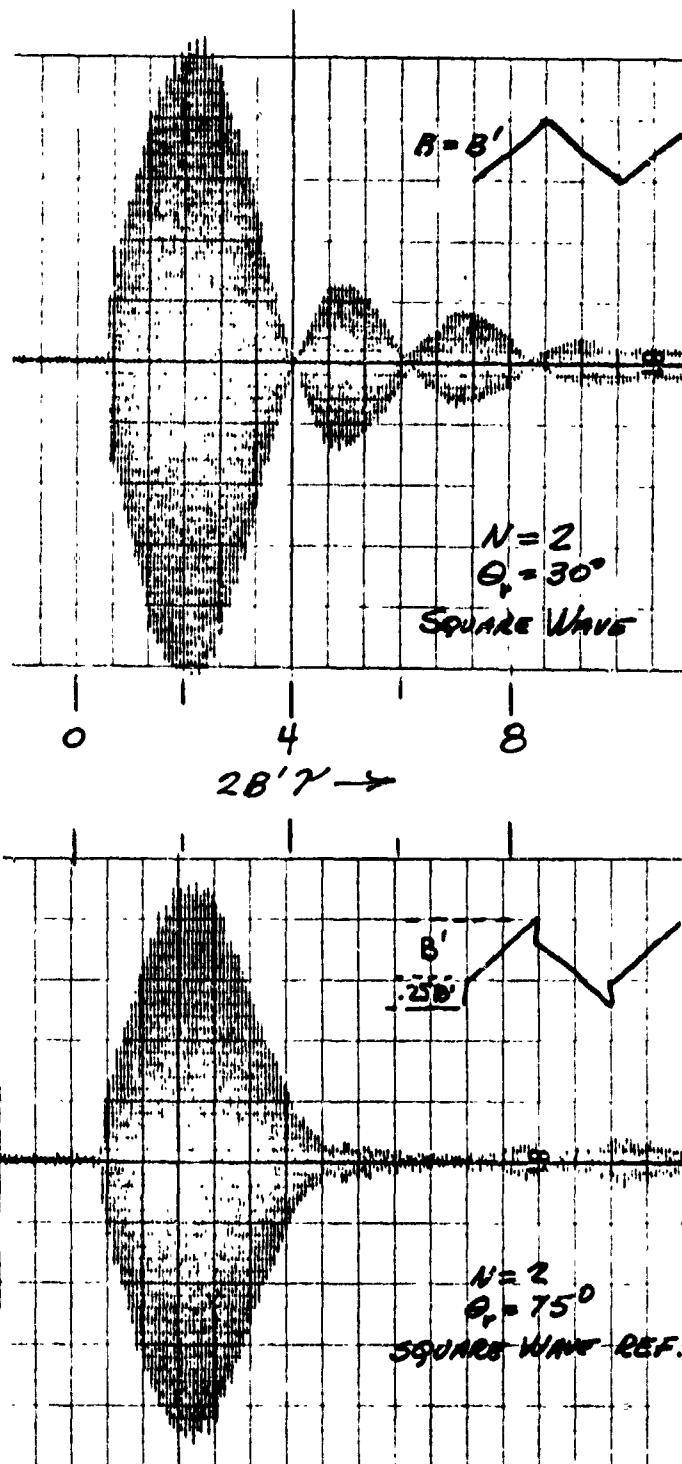
Figure 21. Effect of Square Wave Added to Modulation for N = 2
Range Law (Measured on Exponential Line)
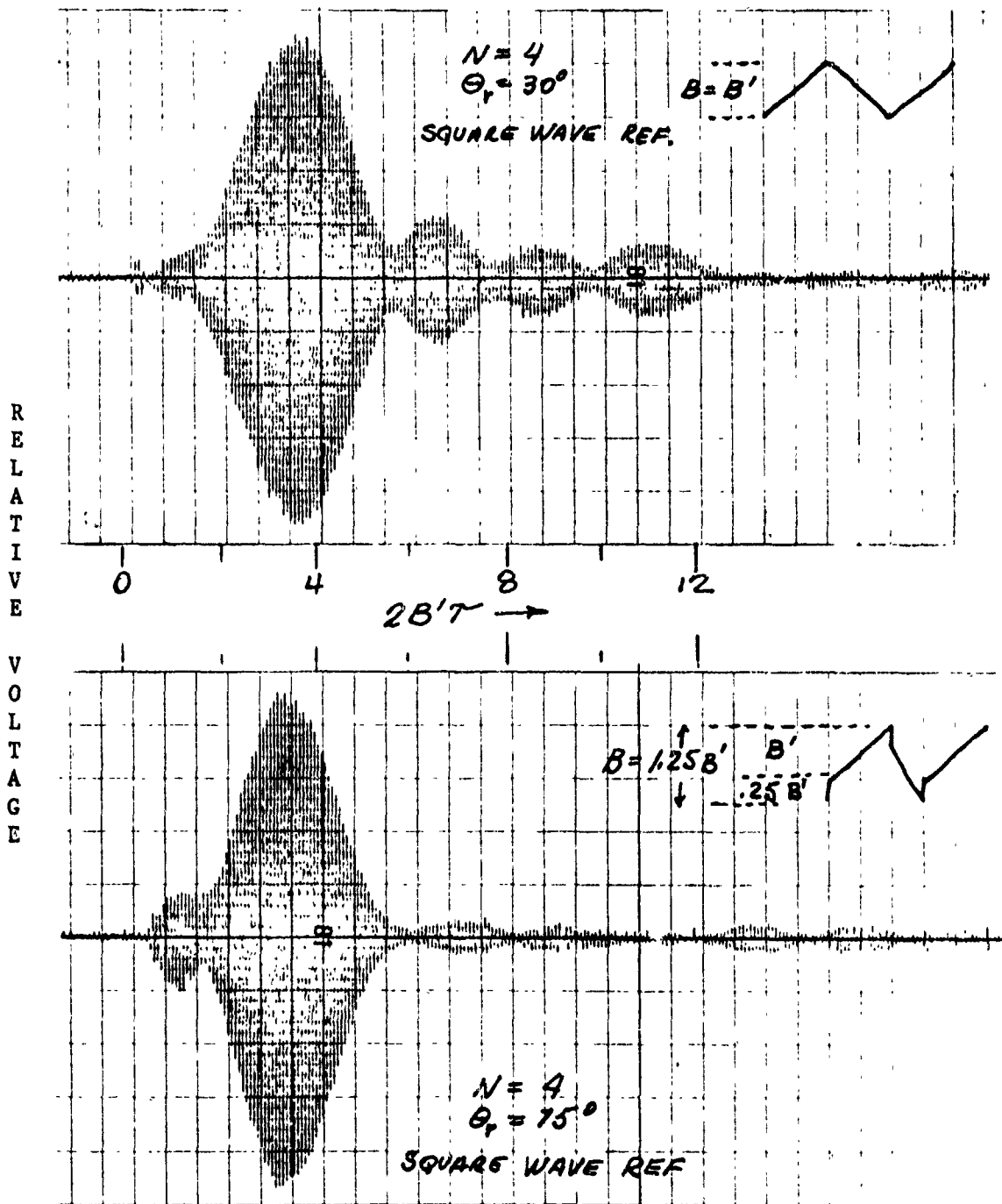
Figure 22.   Effect of Square Wave Added to Modulation for N = 4
             Range Law (Measured on Exponential Line)

REFERENCES

1. Taylor, T.T., "Design of Line-Source Antennas for Narrow Bandwidth and Low Side Lobes," IRE Trans. on Antennas and Propagation, vol. AP-3, pp 16-28, January, 1955.

2. Skolnick, M., Editor, Radar Handbook, McGraw-Hill, 1970.

3. Murakami, T., "Optimum Waveform Study for Coherent Pulse Doppler, RCA Final Report, prepared for Office of Naval Research, Contract No. 4649(00)(x), February 28, 1965. AD 641-391.

4. Couch, L.W., "Effects of Modulation Nonlinearity on the Range Response of FM Radars," IEEE Transactions on Aerospace and Electronic Systems, vol. AES-9, July, 1973.

5. Tozzi, L.M., "Resolution in Frequency-Modulated Radars," Ph.D. Dissertation, University of Maryland, 1972.

6. Couch, L.W., "Range Laws of Distance Measuring Systems Using Frequency Modulation with a Nonlinear Triangular Waveshape," University of Florida Report for Harry Diamond Laboratories, Contract DAAG39-70-C-0058, March 28, 1972. AD 744-483.

7. Rowe, H.E., Signals and Noise in Communications Systems, Van Nostrand, 1965.

8. Rihaczek, A.W., Principles of High Resolution Radar, McGraw-Hill, 1969.

9. McAlpine, G.A., J.F. Dammann, and J.H. Highfill, "Post Mixer Spectra of Periodic FM Altimeters with Area Target Returns," IEEE Trans. on Aerospace and Electronic Systems, vol. AES-7, pp 932-940, Sept. 1971.

10. Helstrom, C.W., Statistical Theory of Signal Detection, Pergamon Press: New York, 1968.

11. Woodward, P.M., Probability and Information Theory with Applications to Radar, McGraw-Hill: New York, 1953.

12. Kalmus, H.P., "Directional Sensitive Doppler Device," Proceedings of the I.R.E., vol. 43, pp 698-700, June, 1955.

13. Kalmus, H.P., "Doppler Wave Recognition with High Clutter Rejection," IEEE Transactions on Aerospace and Electronic Systems, vol. AES-3, pp 334-339, November, 1967.

Accuracy of Piecewise-Linear Approximation

In order to show that the range law for a continuous frequency modulation function approaches that of a piecewise linear approximation of the modulation function, a cosine modulation waveform was approximated by straight line segments and the resulting range law compared to the known nth harmonic range law[2] given by $J_n(\pi B\tau)$.

The appropriate values of ψ_ℓ and ρ_ℓ to be used in (51) were determined as shown below.
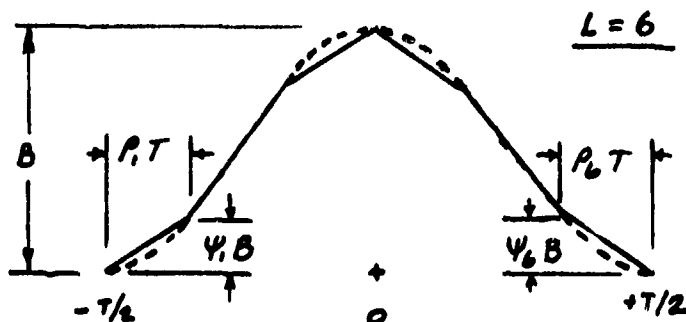
Piecewise Linear Approximation of Cosine Wave
(L Must be an Even Integer $\geq$ 6)

$$\rho_\ell = 1/L$$

$$\psi_\ell = 0.5 \left(\cos\left[2\pi \frac{(\ell-1)}{L}\right] - \cos\left[2\pi\frac{\ell}{L}\right] \right) , \quad \ell = 1, 2 \cdots L$$

The cosine waveform was divided into both 10 and 14 equal time segments and the resulting piecewise linear waveform was then used to compute the range laws shown on Figures 21 to 25. Although the higher harmonic range laws require a larger number of sections for the same degree of accuracy, it is obvious that as the number of sections are increased the computed response more nearly approximates J_n.
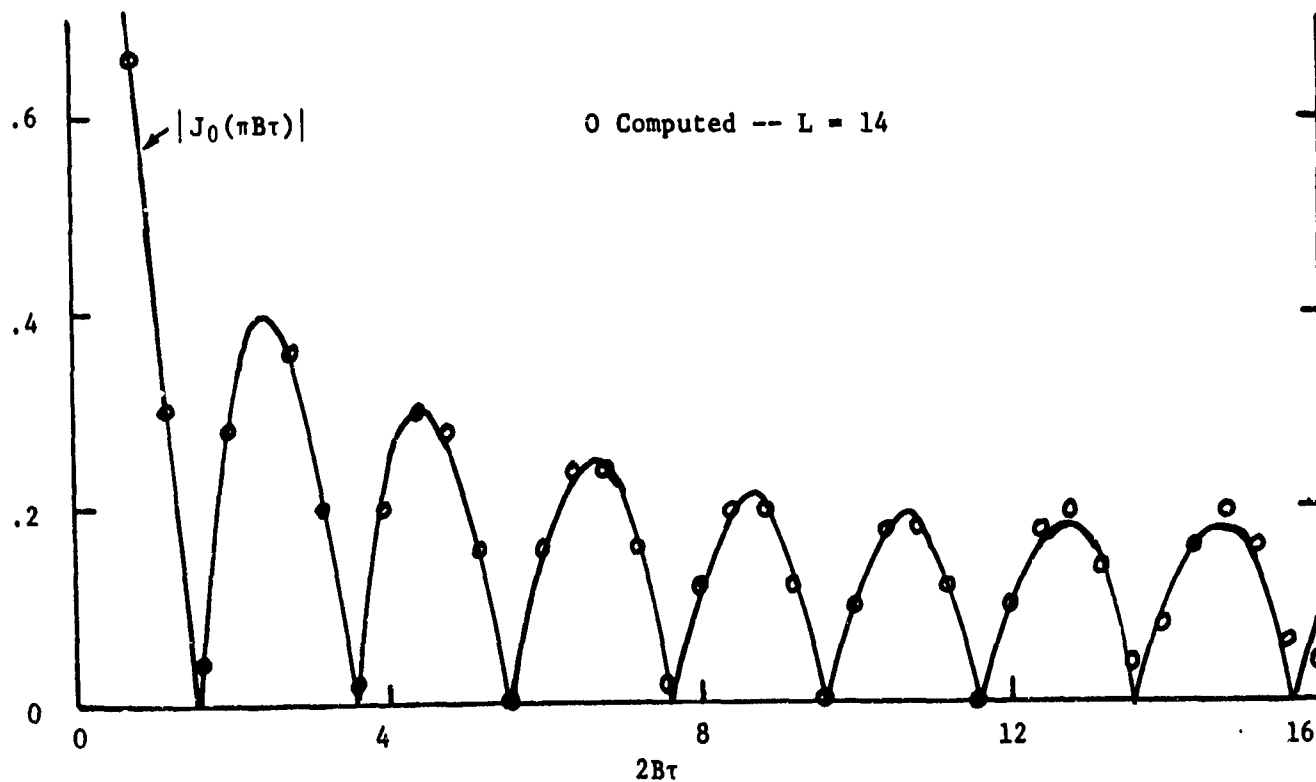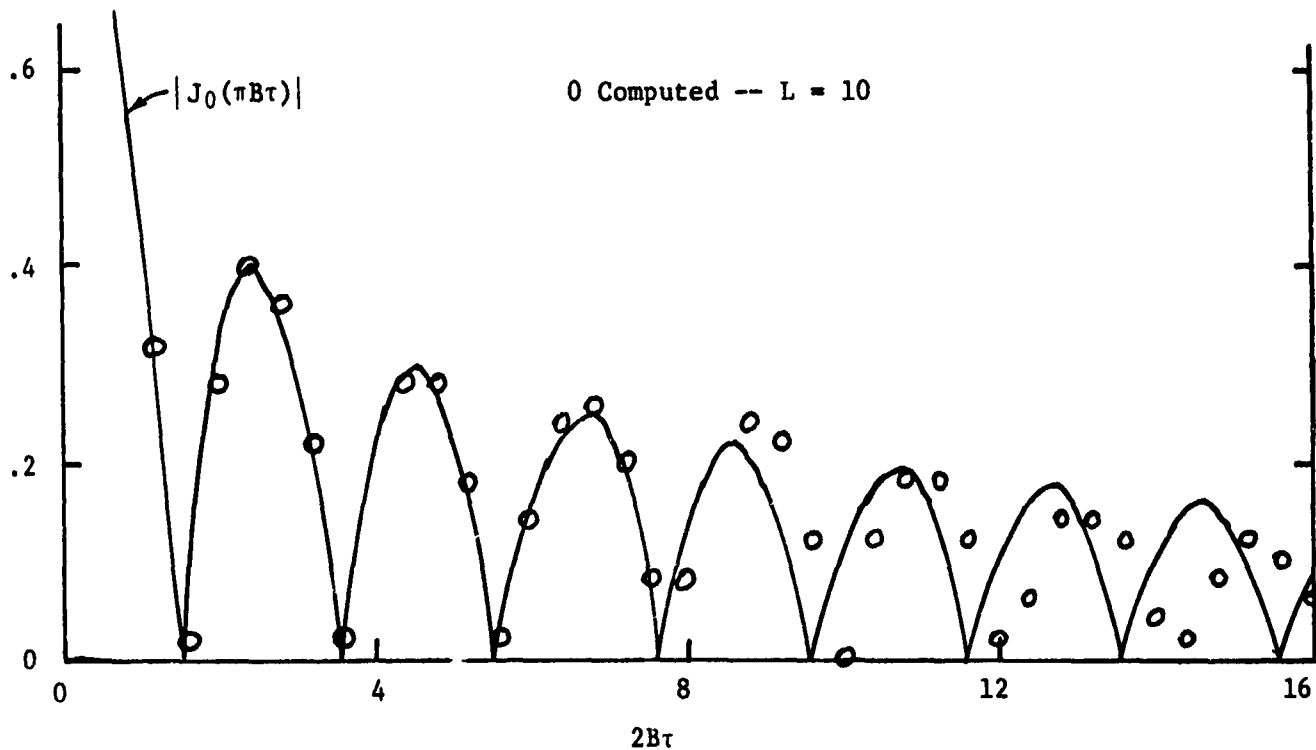
Figure 23. N = 0 Range Law for Ten and Fourteen Section
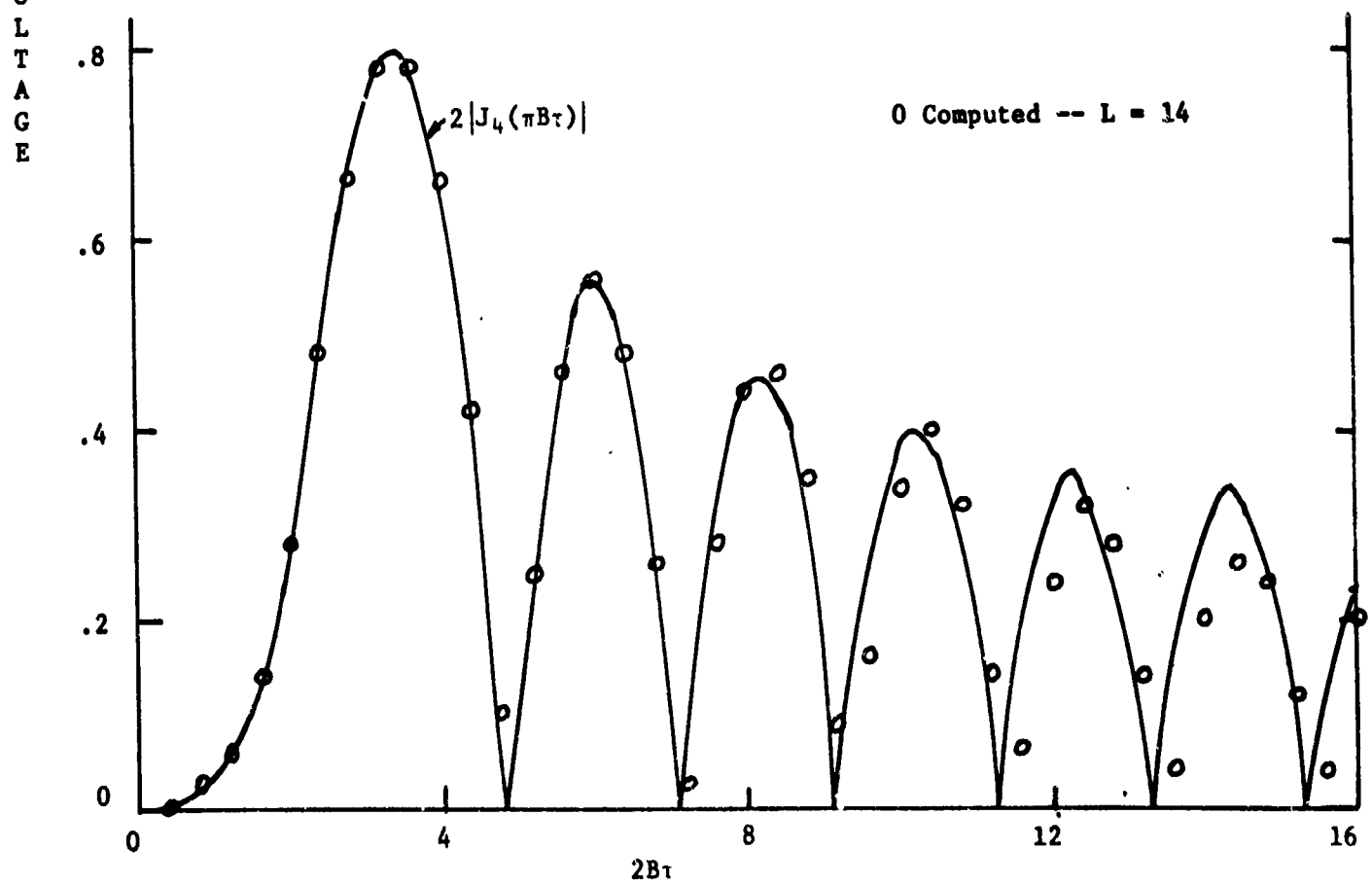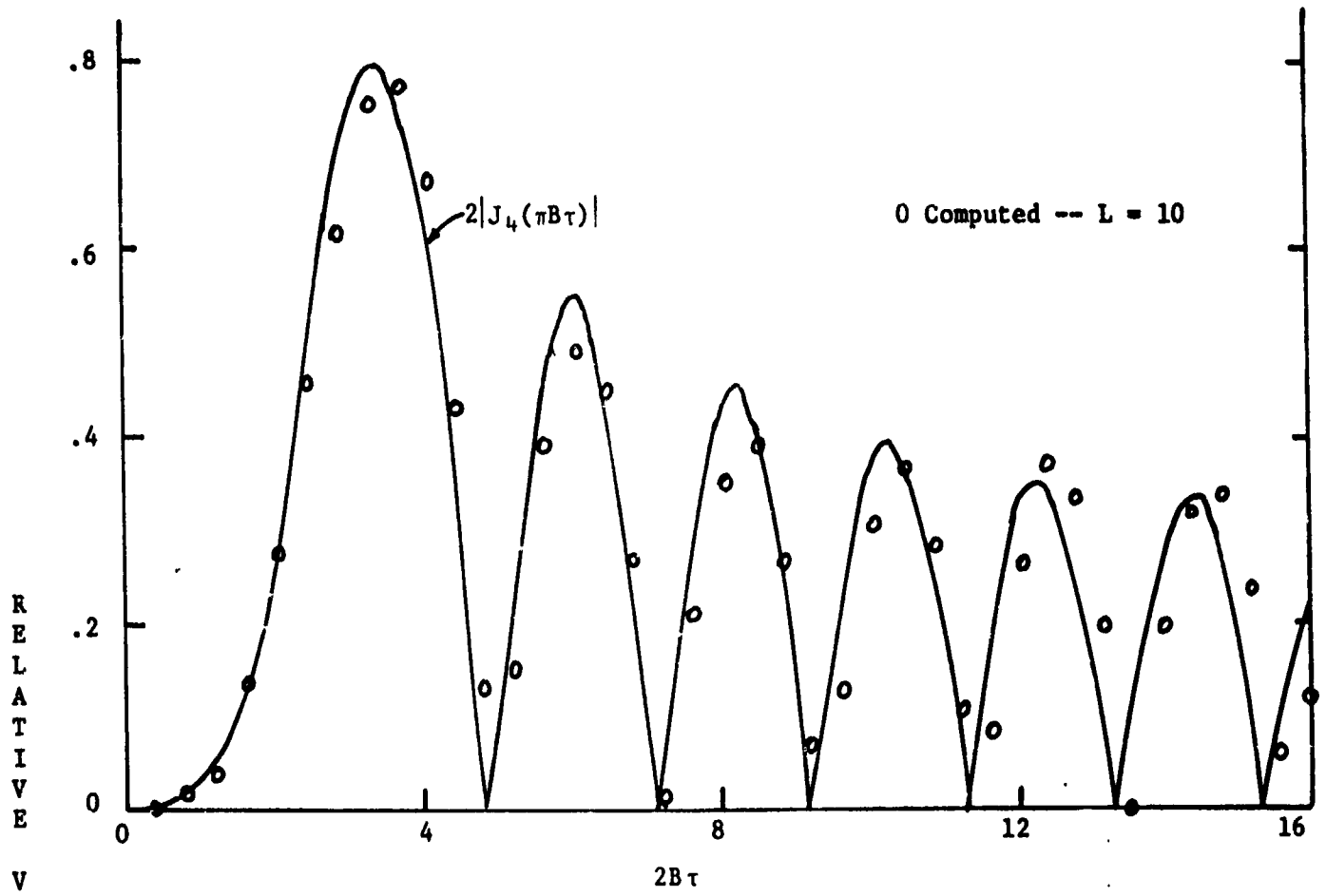Approximation to Sine Wave Modulation

Figure 24. N = 4 Range Law for Ten and Fourteen Section
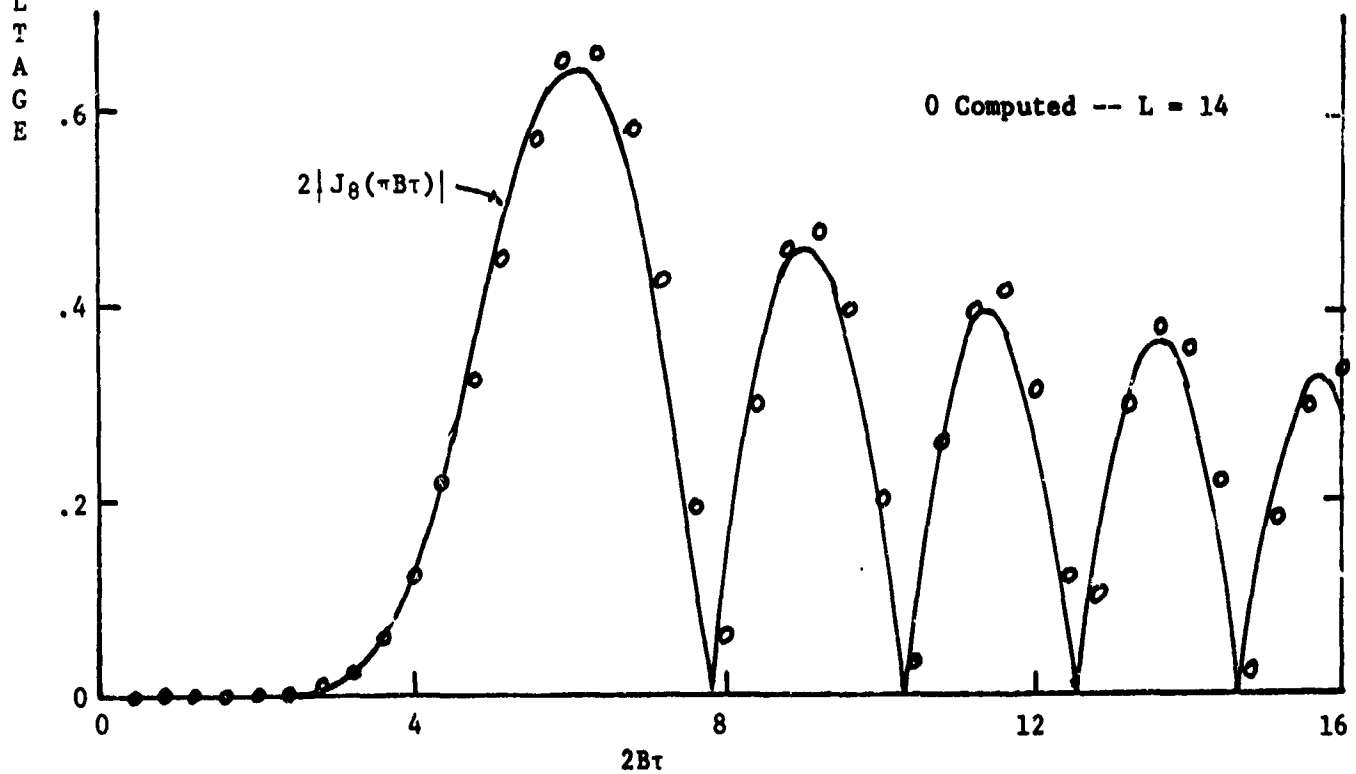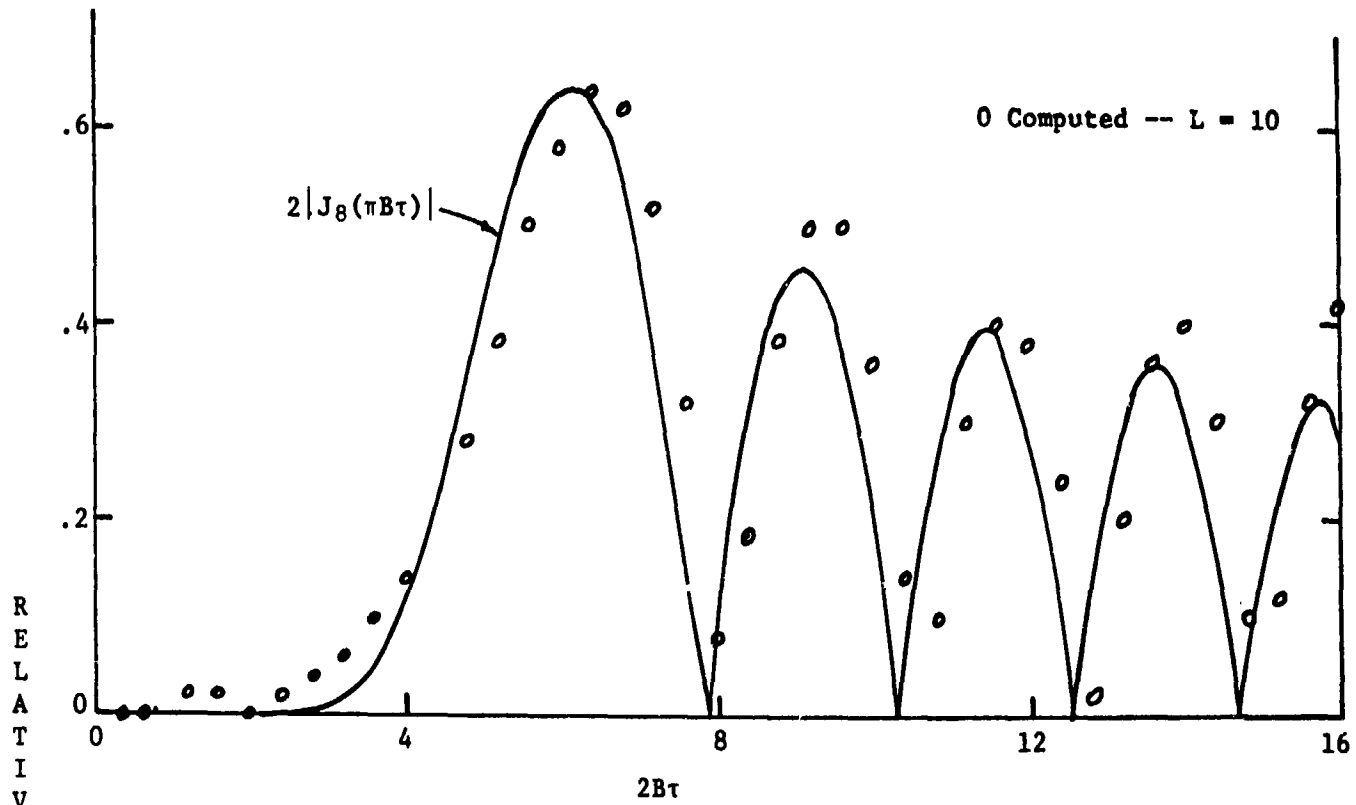Approximation to Sine Wave Modulation

Figure 25. N = 8 Range Law for Ten and Fourteen Section
Approximation to Sine Wave Modulation